

Phase Structures of the Black Dp - $D(p+4)$ -Brane System in Various Ensembles

Da Zhou^{1,a,b}, Zhi-Guang Xiao^{2,a,c}

^a *The Interdisciplinary Center for Theoretical Study,
University of Science and Technology of China,
Hefei, Anhui, 230026, China*

^b *Department of Mathematics, City University London,
London EC1V 0HB, U.K.*

^c *State Key Laboratory of Theoretical Physics,
Institute of Theoretical Physics,
Chinese Academy of Sciences, Beijing 100190, China*

Abstract

When the $D(p+4)$ -brane with delocalized Dp charges is put into equilibrium with a spherical thermal cavity, the two kinds of charges can be put into canonical or grand canonical ensemble independently by setting different conditions at the boundary. We discuss the phase structures of various ensembles of this system formed in this way and find out the conditions that the black brane could be the final stable phase in these ensembles. In particular, van der Waals-like phase transitions can happen when $D0$ and $D4$ charges are in different kinds of ensembles. Furthermore, our results indicate that the $D(p+4)$ -branes and the delocalized Dp -branes are equipotent as far as only thermodynamical phenomena are concerned.

¹Email: da.z.zhou@gmail.com

²Email: xiaozg@ustc.edu.cn

1 Introduction

Branes are non-perturbative objects in String theory and study on them is helpful in the understanding of the non-perturbative properties of String theory. Various brane configurations are also useful in the applications of gauge-string duality. Under the assumption of AdS/CFT, study on the near horizon geometry of D3 brane, i.e. $\text{AdS}_5 \times S^5$, reveals the properties of corresponding strong coupling conformal field theory in the large N_c limit at the boundary of AdS_5 , which can also be extended to the asymptotically AdS_5 spaces. A typical example is that the well-known Hawking-Page phase transition of the AdS black hole corresponds to the confinement-deconfinement phase transition in $SU(N_c)$ gauge theory at large N_c [1], which aroused the recent interests on the black hole thermodynamics in the asymptotically AdS space.

As the solutions of the supergravity, black branes, like black holes, can have their own thermodynamics. Study on the thermodynamical phase structure of the black branes is also valuable in understanding the non-perturbative nature of String theory. Since black branes are asymptotically flat, they are unstable by themselves due to their negative heat capacity and the Hawking radiation. To study their phase structures, one can put them into a spherical cavity which is considered as a reservoir to form a thermal equilibrium, following the approach of York in discussing the thermodynamics of black holes[2, 3, 4]. For different boundary conditions at the boundary of the cavity, there can be different ensembles for charged black branes. Along these lines, in [5], the phase structure of black p -branes in the canonical ensemble was studied in D -dimensional space-time, where the temperature, the volume of the brane as well as the cavity, and the charges of the brane are fixed. There can be van der Waals-like phase transition in this system for $\tilde{d} > 2$ ($p < 5$) where $D = d + \tilde{d} + 2$ and $p = d - 1$: a first order phase transition between a large black brane and a small one can be found for charge $q < q_c$, while for $q > q_c$ there is only one black brane phase, with q_c being the critical charge at which there is a second order phase transition. This is similar to the van der Waals-like phase transition found in charged AdS black holes [6, 7], asymptotically flat black holes as well as dS black holes [8, 9]. In contrast, for $\tilde{d} \leq 2$ ($p = 5, 6$), there is no van der Waals-like phase transition. For uncharged black branes, Hawking-Page like transitions between black branes and the “hot flat space” can also happen in the canonical ensemble similar to the uncharged black hole case [2, 3]. The phase structure for black branes in grand canonical ensemble is different from that in canonical ensemble for $\tilde{d} > 2$, where the potential is fixed while the charges are not. There is no van der Waals-like phase transition, but the Hawking-Page-like transitions between the black branes and the “hot flat space” can happen. Bubble solutions[10, 11] which can be obtained from black branes by double wick rotations also play a role in the phase structure of black branes, since they have the same boundary condition as the black branes. In [12] and [13], bubbles were found to be the phases of black branes in canonical ensembles and grand canonical ensembles, and can have phase transitions with black branes, and thus enriches the phase structure of black branes. In all these discussions, there are no van der Waals-like phase transitions in grand canonical ensembles, whereas they do exist in canonical ensembles. The absence of van der Waals-like phase transitions in grand canonical ensemble is also true for charged black holes either in

flat space[4, 8] or in AdS space [6, 7], but they may exist for Gauss-Bonnet AdS black holes[14, 15, 16] for certain Gauss-Bonnet coupling constants.

It is well-known that branes can be combined to form composite states or intersecting branes. Among others, Dp - $D(p+4)$ bound states as solutions of supergravities can be constructed by smearing Dp branes inside $D(p+4)$ branes. In extremal cases[17, 18, 19] which obey the harmonic function rules, the solutions preserve 1/4 of the supersymmetries. There can also be more generic non-supersymmetric Dp - $D(p+4)$ solutions in ten-dimensional supergravities[20, 21]. These brane solutions are useful in gravity-gauge duality applications[22, 23, 24, 25, 26, 27] and in constructing lower dimensional black holes[20]. The dynamical stability of Dp - $D(p+4)$ was discussed in[28]. We are interested in the thermodynamical phase structure of these solutions in this paper. Since these solutions involve two kinds of charges coupled with different RR potentials, the phase structure is expected to be richer. One can form different ensembles by fixing either the charge inside the cavity or the potential at the boundary for Dp or/and $D(p+4)$ branes, and therefore Dp and $D(p+4)$ can be in canonical ensemble or in grand canonical ensemble independently. In [29], the phase structure of the D1-D5 system in which both branes are in the canonical ensemble is discussed. It has been shown that the smeared D1-brane alone shares the same phase structure as the D5-brane for which the van der Waals-like phase structure can not be found. However the D1-D5 combined system displays a van der Waals-like phase structure for some region of the charge combinations. And the phase structure is also symmetric under the exchange of the D1 charges and D5 charges. One may also be curious about what will happen when the two kinds of charges are in different ensembles. In present paper we will study the phase structures of the other three combinations of the ensembles: both Dp and $D(p+4)$ in grand canonical ensemble, Dp in canonical and $D(p+4)$ in grand canonical ensemble, and Dp in grand canonical and $D(p+4)$ in canonical ensemble. We will find that the phase structures are also symmetric when one swaps the boundary conditions imposed on Dp - and $D(p+4)$ -branes. For mixed ensembles with one charge in canonical ensemble and the other in grand canonical ensemble, one may expect in some charge combinations there could be van der Waals-like phase transitions like the canonical ensemble and in some other regions there are no van der Waals-like phase transitions as in grand canonical ensemble. This indeed happens in the D0-D4 system, which has the richest phase structure. In D2-D6 and D1-D5 systems, unlike in the D1-D5 canonical ensemble, in the other three ensembles there are still no van der Waals-like phase transitions.

The paper is organized as follows. In section 2, we review the Dp - $D(p+4)$ solution and evaluate the classical Euclidean actions or thermodynamic potentials for different ensembles. In section 3, we discuss the phase structures of the Dp - $D(p+4)$ system in different ensembles. Section 4 is the conclusion. We also gather some detailed calculations in the Appendices.

2 The Dp-D(p + 4) brane system

2.1 The action

We consider a gravitational system bounded by a big spherical reservoir which can be regarded as a spherical boundary at the transverse radius ρ_b . At the center of the system is a pile of parallel Dp-D(p + 4)-branes. The total Euclidean 10-dimensional supergravity action in Einstein frame can be expressed as a sum of several contributions [5],

$$I = I_{\text{EH}} + I_\phi + I_p + I_{p+4} + I_{\text{boundary}} \quad (1)$$

where the first term is the usual Einstein-Hilbert action,

$$I_{\text{EH}} = -\frac{1}{2\kappa^2} \int d^{10}x \sqrt{g} R, \quad (2)$$

the second term is the contribution from the dilaton field,

$$I_\phi = \frac{1}{4\kappa^2} \int d^{10}x \sqrt{g} \partial^\mu \phi \partial_\mu \phi, \quad (3)$$

the third and fourth terms come from the Dp- and D(p + 4)-brane form field action,

$$\begin{aligned} I_p &= \frac{1}{4\kappa^2} \int d^{10}x \sqrt{g} \frac{e^{a_p \phi}}{(p+2)!} F_{[p+2]}^2, \\ I_{p+4} &= \frac{1}{4\kappa^2} \int d^{10}x \sqrt{g} \frac{e^{a_{p+4} \phi}}{(p+6)!} F_{[p+6]}^2, \end{aligned} \quad (4)$$

where $a_n = \frac{3-n}{2}$, and the last term I_{boundary} could admit several boundary integration terms, which depends on what ensemble we are interested in. We will come back to this term soon. In the above formulae, the constant coefficient κ is defined as $\kappa = \sqrt{8\pi G_{10}^2}$ in which G_{10} is the 10-dimensional Newton's constant; the vacuum expectation value of the dilaton field $\phi(r \rightarrow \infty)$ has been shifted to zero. The integration is performed within the boundary and outside the horizon if there exists one.

Now we deal with the boundary term in equation (1). There are three terms that may contribute to the boundary action I_{boundary} ,

$$\begin{aligned} I_{\text{GH}} &= \frac{1}{\kappa^2} \oint d^9x \sqrt{\gamma} (K - K_0), \\ I_{b,p} &= -\frac{1}{2\kappa^2} \oint d^9x \sqrt{\gamma} \frac{e^{a_p \phi}}{(p+1)!} n_\mu F^{\mu\nu_1 \dots \nu_{p+1}} A_{\nu_1 \dots \nu_{p+1}}, \\ I_{b,p+4} &= -\frac{1}{2\kappa^2} \oint d^9x \sqrt{\gamma} \frac{e^{a_{p+4} \phi}}{(p+5)!} n_\mu F^{\mu\nu_1 \dots \nu_{p+5}} A_{\nu_1 \dots \nu_{p+5}}. \end{aligned} \quad (5)$$

The first action above is the Gibbons-Hawking surface term [30], in which K is the trace of the extrinsic curvature $K_{\mu\nu}$ defined as

$$K_{\mu\nu} = -\frac{1}{2} (\nabla_\mu n_\nu + \nabla_\nu n_\mu) \quad (6)$$

where n_μ is the normalized space-like vector normal to the boundary. K_0 in that term is defined in the same manner as K but with the metric replaced with flat metric. This subtraction term is included to make I_{GH} vanish for flat metric [30]. The second and third actions in (5) are boundary contributions from the Dp - and $D(p+4)$ -branes respectively. γ in these equations is the determinant of the induced metric on the $(4-p)$ -dimensional boundary, and the $(p+1)$ -form and $(p+5)$ -form fields $A_{[p+1]}$ and $A_{[p+5]}$ are the Ramond-Ramond potentials of Dp - and $D(p+4)$ -branes respectively.

The Gibbons-Hawking term should always be included in I_{boundary} regardless of what ensemble we are talking about. However, $I_{b,p}$ and $I_{b,p+4}$ are supposed to cancel additional boundary terms when doing variations with respect to the gauge field potentials. If we fix the gauge field strength F on the boundary and the potential A are not fixed, after partial integration the additional boundary terms would emerge, thus we need to include $I_{b,p}$ or $I_{b,p+4}$ whose variations would cancel these terms. On the other hand, if we fix the gauge potential A on the boundary, there will be no additional variation terms, therefore, $I_{b,p}$ or $I_{b,p+4}$ will not be needed. We summarize the above analyses in Table 1. The

Dp	$D(p+4)$	Boundary action I_{boundary}
Fixing $A_{[p+1]}$	Fixing $A_{[p+5]}$	I_{GH}
Fixing $F_{[p+2]}$	Fixing $A_{[p+5]}$	$I_{\text{GH}} + I_{b,p}$
Fixing $A_{[p+1]}$	Fixing $F_{[p+6]}$	$I_{\text{GH}} + I_{b,p+4}$
Fixing $F_{[p+2]}$	Fixing $F_{[p+6]}$	$I_{\text{GH}} + I_{b,p} + I_{b,p+4}$

Table 1: The relationship between boundary conditions and the boundary action

relation between boundary conditions and ensembles will be addressed in next subsection.

2.2 Black brane solution

The generic non-supersymmetric Dp - $D(p+4)$ brane solution [20, 21, 28] can be obtained by directly solving the supergravity equations of motion or by a series of duality and boost operations from $D(p+4)$ -branes. We use following coordinates to describe the solution,

$$(t, x_1, \dots, x_p, \dots, x_{p+4}, \rho, \phi_1, \dots, \phi_{4-p}) \quad (7)$$

where ρ is the radius in the transverse directions perpendicular to x_m , $m = 1, \dots, p+4$. In this coordinates the solution reads [29],

$$\begin{aligned}
ds^2 &= \Delta_-^{\frac{1-p}{4}} \Delta_*^{\frac{p-7}{8}} \left(\Delta_+ dt^2 + \Delta_- \sum_{i=1}^p dx_i^2 + \Delta_* \sum_{j=p+1}^{p+4} dx_j^2 \right) \\
&\quad + \Delta_-^{\frac{p^2-1}{4(3-p)}} \Delta_*^{\frac{p+1}{8}} \left(\frac{d\rho^2}{\Delta_+ \Delta_-} + \rho^2 d\Omega_{4-p}^2 \right), \\
e^\phi &= \Delta_-^{\frac{p-1}{2}} \Delta_*^{\frac{3-p}{4}}, \\
A_{[p+1]} &= -i \frac{\Delta_+}{\Delta_*} \left(\frac{\Delta_* - \Delta_-}{\Delta_* - \Delta_+} \right)^{1/2} dt \wedge dx_1 \wedge \dots \wedge dx_p, \\
F_{[p+2]} &= i \frac{3-p}{\rho} \frac{1}{\Delta_*} \left(1 - \frac{\Delta_+}{\Delta_*} \right)^{1/2} \left(1 - \frac{\Delta_-}{\Delta_*} \right)^{1/2} dt \wedge d\rho \wedge dx_1 \wedge \dots \wedge dx_p, \\
A_{[p+5]} &= -i \Delta_+ \left(\frac{1 - \Delta_-}{1 - \Delta_+} \right)^{1/2} dt \wedge dx_1 \wedge \dots \wedge dx_{p+4}, \\
F_{[p+6]} &= i \frac{3-p}{\rho} (1 - \Delta_+)^{1/2} (1 - \Delta_-)^{1/2} dt \wedge d\rho \wedge dx_1 \wedge \dots \wedge dx_{p+4}, \tag{8}
\end{aligned}$$

where

$$\begin{aligned}
\Delta_\pm(\rho) &= 1 - \frac{\rho_\pm^{3-p}}{\rho^{3-p}}, \quad \rho_+ > \rho_- \geq 0, \\
\Delta_*(\rho) &= 1 - \frac{k}{\rho^{3-p}}, \quad \rho_-^{3-p} \geq k > -\infty. \tag{9}
\end{aligned}$$

Here, p can be 0, 1, 2 for this supergravity solution to describe the D p -D($p+4$) system. The constants ρ_+ and ρ_- are the coordinates for the outer event horizon and an inner event horizon respectively, the latter being a curvature singularity. Therefore, the requirement $\rho_+ > \rho_-$ is to avoid a naked curvature singularity. The other constant k can be either positive or negative, and when it is positive, there is another inner event horizon at $\rho = k^{1/(3-p)}$ which is a curvature singularity as well. When $k = \rho_-^{3-p}$, we have $\Delta_* = \Delta_-$, and this corresponds to the brane configuration where all D p -branes are removed from the system while D($p+4$)-branes are retained. Later we will see in (11) that we require $\rho_-^{3-p} \geq k$ in order to make the Ramond-Ramond charge real.

The D p - and D($p+4$)-brane charge densities can be obtained by integrating the Hodge dual of their Ramond-Ramond field strengths,

$$\begin{aligned}
\mathcal{Q}_p &= \frac{-i}{\sqrt{2}\kappa} \int_{x_{p+1}, \dots, x_{p+4}} \int_{S^{4-p}} e^{a_p \bar{\phi}} * F_{[p+2]}(\rho_b), \\
\mathcal{Q}_{p+4} &= \frac{-i}{\sqrt{2}\kappa} \int_{S^{4-p}} e^{a_{p+4} \bar{\phi}} * F_{[p+6]}(\rho_b), \tag{10}
\end{aligned}$$

where $\bar{\phi} \equiv \phi(\rho_b)$ and the $-i$ factors come from Euclideanization. The charge densities can be explicitly

expressed as follows,

$$\begin{aligned}\mathcal{Q}_p &= \frac{(3-p)V_4\Omega_{4-p}}{\sqrt{2}\kappa} e^{a_p\bar{\phi}/2} \bar{\rho}_b^{3-p} \left(1 - \frac{\bar{\Delta}_+}{\bar{\Delta}_*}\right)^{1/2} \left(1 - \frac{\bar{\Delta}_-}{\bar{\Delta}_*}\right)^{1/2}, \\ \mathcal{Q}_{p+4} &= \frac{(3-p)\Omega_{4-p}}{\sqrt{2}\kappa} e^{a_{p+4}\bar{\phi}/2} (\bar{\rho}_+ \bar{\rho}_-)^{\frac{3-p}{2}},\end{aligned}\quad (11)$$

where

$$V_4 = \sqrt{g_{x_{p+1}x_{p+1}}(\rho_b) \cdots g_{x_{p+4}x_{p+4}}(\rho_b)} V_4^*, \quad V_4^* \equiv \int dx_{p+1} \cdots dx_{p+4},$$

and

$$\begin{aligned}\bar{\Delta}_\pm &\equiv \Delta_\pm(\rho_b) = 1 - \frac{\bar{\rho}_\pm^{3-p}}{\rho_b^{3-p}}, \\ \bar{\Delta}_* &\equiv \Delta_*(\rho_b) = 1 - \frac{\bar{k}}{\rho_b^{3-p}},\end{aligned}\quad (12)$$

in which

$$\bar{\rho}_{+,-,b} \equiv \rho_{+,-,b} \bar{\Delta}_-^{\frac{p^2-1}{8(3-p)}} \bar{\Delta}_*^{\frac{p+1}{16}} = \rho_{+,-,b} e^{\frac{p+1}{4(3-p)}\bar{\phi}} \quad (13)$$

are the physical radii of horizons and the boundary, and $\bar{k} \equiv k e^{\frac{p+1}{4}\bar{\phi}}$.

To make these relations more concise, we define two reduced charge densities,

$$\begin{aligned}\tilde{\mathcal{Q}}_p &= \frac{\sqrt{2}\kappa\mathcal{Q}_p e^{-a_p\bar{\phi}/2}}{(3-p)V_4\Omega_{4-p}\bar{\rho}_b^{3-p}} \\ &= \left(1 - \frac{\bar{\Delta}_+}{\bar{\Delta}_*}\right)^{1/2} \left(1 - \frac{\bar{\Delta}_-}{\bar{\Delta}_*}\right)^{1/2} < 1, \\ \tilde{\mathcal{Q}}_{p+4} &= \left(\frac{\sqrt{2}\kappa\mathcal{Q}_{p+4} e^{-a_{p+4}\bar{\phi}/2}}{(3-p)\Omega_{4-p}}\right)^{\frac{1}{3-p}} = \sqrt{\bar{\rho}_+ \bar{\rho}_-}.\end{aligned}\quad (14)$$

With (14) we can express $\bar{\rho}_-$ and $\bar{\Delta}_*$ through $\bar{\rho}_+$ and these two reduced quantities,

$$\begin{aligned}\bar{\rho}_- &= \frac{\tilde{\mathcal{Q}}_{p+4}^2}{\bar{\rho}_+}, \\ \bar{\Delta}_* &= \frac{\bar{\Delta}_+ + \bar{\Delta}_- \pm \sqrt{(\bar{\Delta}_- - \bar{\Delta}_+)^2 + 4\tilde{\mathcal{Q}}_p^2 \bar{\Delta}_+ \bar{\Delta}_-}}{2(1 - \tilde{\mathcal{Q}}_p^2)}.\end{aligned}\quad (15)$$

When $k = \rho_-^{3-p}$, the Dp-brane charge vanishes and $\tilde{\mathcal{Q}}_p = 0$, so

$$\bar{\Delta}_* = \frac{\bar{\Delta}_+ + \bar{\Delta}_- \pm (\bar{\Delta}_- - \bar{\Delta}_+)}{2} = \bar{\Delta}_-.$$

Therefore, we should choose in the above relation the “+” sign only, i.e.,

$$\bar{\Delta}_* = \frac{\bar{\Delta}_+ + \bar{\Delta}_- + \sqrt{(\bar{\Delta}_- - \bar{\Delta}_+)^2 + 4\tilde{\mathcal{Q}}_p^2 \bar{\Delta}_+ \bar{\Delta}_-}}{2(1 - \tilde{\mathcal{Q}}_p^2)}.\quad (16)$$

Dp-brane	D(p + 4)-brane	Boundary action I_{boundary}
Canonical	Canonical	$I_{\text{GH}} + I_{b,p} + I_{b,p+4}$
Grand Canonical	Canonical	$I_{\text{GH}} + I_{b,p+4}$
Canonical	Grand Canonical	$I_{\text{GH}} + I_{b,p}$
Grand Canonical	Grand Canonical	I_{GH}

Table 2: The relationship between ensembles and the boundary action

From (11), we can see that fixing F at the boundary is to fix the charge density \mathcal{Q} within the boundary. It is well-known that fixing the charge of a system while allowing radiation means we are considering the system in canonical ensemble. If we fix the gauge potential A instead, the field strength at the boundary will be changeable, and we will be talking about grand canonical ensemble. Now that we have two kinds of gauge potentials and field strengths, it is reasonable to assume there are two kinds of ensembles for each field, and thus we have the following table (Table 2).

2.3 Temperature and conjugate potentials

Like black holes, due to Hawking radiation [31], black brane has a temperature, T_H , which can be easily calculated by the requirement that the Euclideanized metric (8) has no conical singularity. Then the Euclideanized time t is cyclic with a particular period

$$\beta^* = \frac{4\pi\rho_b (1 - \bar{\Delta}_+)^{1/2} (\bar{\Delta}_* - \bar{\Delta}_+)^{1/2}}{3 - p (\bar{\Delta}_- - \bar{\Delta}_+)^{\frac{2-p}{3-p}}}. \quad (17)$$

This period is just the inverse of the Hawking temperature observed by an observer at $\rho = \infty$,

$$T_H = 1/\beta^*. \quad (18)$$

For a local observer at $\rho = \rho_b$, the local temperature would be

$$\bar{\beta} = \beta^* \bar{\Delta}_+^{\frac{1}{2}} \bar{\Delta}_-^{\frac{1-p}{8}} \bar{\Delta}_*^{\frac{p-7}{16}} = \frac{4\pi\bar{\rho}_b}{3-p} (1 - \bar{\Delta}_+)^{\frac{1}{2}} \left(\frac{\bar{\Delta}_+}{\bar{\Delta}_-}\right)^{\frac{1}{2}} \left(1 - \frac{\bar{\Delta}_+}{\bar{\Delta}_-}\right)^{\frac{p-2}{3-p}} \left(1 - \frac{\bar{\Delta}_+}{\bar{\Delta}_*}\right)^{\frac{1}{2}}. \quad (19)$$

In order to study the grand canonical ensembles, we need to define two potentials which are conjugate to the brane charge densities. So we define Φ_p to be the potential conjugate to the Dp charge using

$$A_{[n+1]} = -i\sqrt{2}\kappa \Phi_n d\bar{t} \wedge d\bar{x}_1 \wedge \cdots \wedge d\bar{x}_n, \quad (20)$$

where the barred coordinates are defined as follows,

$$\begin{aligned} \bar{t} &= t \bar{\Delta}_+^{\frac{1}{2}} \bar{\Delta}_-^{\frac{1-p}{8}} \bar{\Delta}_*^{\frac{p-7}{16}}, \\ \bar{x}_i &= x_i \bar{\Delta}_-^{\frac{5-p}{8}} \bar{\Delta}_*^{\frac{p-7}{16}}, \quad i = 1, \dots, p, \\ \bar{x}_j &= x_j \bar{\Delta}_-^{\frac{1-p}{8}} \bar{\Delta}_*^{\frac{p+1}{16}}, \quad j = p+1, \dots, p+4. \end{aligned} \quad (21)$$

The reasonableness of the definition of the conjugate potentials will be justified later. At the boundary, in the equilibrium state, Φ_p and Φ_{p+4} can be expressed using $\bar{\Delta}_{+,-,*}$ explicitly according to (8),

$$\begin{aligned}\Phi_p &= \frac{1}{\sqrt{2\kappa}} e^{-a_p \bar{\phi}/2} \left(\frac{\bar{\Delta}_+}{\bar{\Delta}_-} \right)^{1/2} \left(\frac{\bar{\Delta}_* - \bar{\Delta}_-}{\bar{\Delta}_* - \bar{\Delta}_+} \right)^{1/2}, \\ \Phi_{p+4} &= \frac{1}{\sqrt{2\kappa}} e^{-a_{p+4} \bar{\phi}/2} \left(\frac{\bar{\Delta}_+}{\bar{\Delta}_-} \right)^{1/2} \left(\frac{1 - \bar{\Delta}_-}{1 - \bar{\Delta}_+} \right)^{1/2}.\end{aligned}\quad (22)$$

2.4 Evaluation of actions

Since the bulk action terms and the Gibbons-Hawking term in the total action (1) are the common parts that appear in every ensemble, we define their sum as

$$I_c = I_{\text{EH}} + I_\phi + I_p + I_{p+4} + I_{\text{GH}} \quad (23)$$

for later convenience. Using the solution (8) one can evaluate the actions,

$$\begin{aligned}I_c &= -\frac{\bar{\beta} V_{p+4} \Omega_{4-p}}{2\kappa^2} \bar{\rho}_b^{3-p} \left[(5-p) \left(\frac{\bar{\Delta}_+}{\bar{\Delta}_-} \right)^{\frac{1}{2}} + (3-p) \left(\frac{\bar{\Delta}_-}{\bar{\Delta}_+} \right)^{\frac{1}{2}} - 2(4-p) \right] \\ &= -\frac{\bar{\beta} V_{p+4} \Omega_{4-p}}{\kappa^2} \bar{\rho}_b^{3-p} \left[(4-p) \left(\frac{\bar{\Delta}_+}{\bar{\Delta}_-} \right)^{\frac{1}{2}} - (4-p) \right] - S, \\ I_{b,p} &= -\frac{\bar{\beta} V_{p+4} \Omega_{4-p}}{2\kappa^2} \bar{\rho}_b^{3-p} \left[(3-p) \frac{(\bar{\Delta}_+ \bar{\Delta}_-)^{\frac{1}{2}}}{\bar{\Delta}_*} - (3-p) \left(\frac{\bar{\Delta}_+}{\bar{\Delta}_-} \right)^{\frac{1}{2}} \right] = \bar{\beta} V_p \mathcal{Q}_p \Phi_p, \\ I_{b,p+4} &= -\frac{\bar{\beta} V_{p+4} \Omega_{4-p}}{2\kappa^2} \bar{\rho}_b^{3-p} \left[(3-p) (\bar{\Delta}_+ \bar{\Delta}_-)^{\frac{1}{2}} - (3-p) \left(\frac{\bar{\Delta}_+}{\bar{\Delta}_-} \right)^{\frac{1}{2}} \right] = \bar{\beta} V_{p+4} \mathcal{Q}_{p+4} \Phi_{p+4},\end{aligned}\quad (24)$$

where

$$S = \frac{2\pi V_{p+4} \Omega_{4-p}}{\kappa^2} \bar{\rho}_b^{4-p} (1 - \bar{\Delta}_+)^{\frac{1}{2}} \left(1 - \frac{\bar{\Delta}_+}{\bar{\Delta}_-} \right)^{\frac{1}{3-p}} \left(1 - \frac{\bar{\Delta}_+}{\bar{\Delta}_*} \right)^{\frac{1}{2}} \quad (25)$$

is the entropy of the brane system and

$$V_{p+4} = V_p V_4, \quad V_p = \sqrt{g_{x_1 x_1}(\rho_b) \cdots g_{x_p x_p}(\rho_b)} V_p^*, \quad V_p^* = \int dx_1 \cdots dx_p. \quad (26)$$

With the above results and Table 2, we obtain the classical actions for various ensembles:

- Both charges are in canonical ensembles (we will use CC ensemble to denote this one)

$$\begin{aligned}I_{CC} &= I_c + I_{b,p} + I_{b,p+4} \\ &= -\frac{\bar{\beta} V_{p+4} \Omega_{4-p}}{2\kappa^2} \bar{\rho}_b^{3-p} \left[2 \left(\frac{\bar{\Delta}_+}{\bar{\Delta}_-} \right)^{\frac{1}{2}} + (3-p) (\bar{\Delta}_+ \bar{\Delta}_-)^{\frac{1}{2}} \left(1 + \frac{1}{\bar{\Delta}_*} \right) + 2p - 8 \right] - S \\ &= \bar{\beta} E - S,\end{aligned}\quad (27)$$

where

$$E = -\frac{V_{p+4}\Omega_{4-p}}{2\kappa^2}\bar{\rho}_b^{3-p}\left[2\left(\frac{\bar{\Delta}_+}{\bar{\Delta}_-}\right)^{\frac{1}{2}}+(3-p)(\bar{\Delta}_+\bar{\Delta}_-)^{\frac{1}{2}}\left(1+\frac{1}{\bar{\Delta}_*}\right)+2p-8\right] \quad (28)$$

is the internal energy of the brane system. This action has already been obtained in [29], and we include it here for completeness.

- Dp in grand canonical ensemble & $D(p+4)$ in canonical ensemble (denoted as GC ensemble)

$$I_{GC} = \bar{\beta}E - S - \bar{\beta}V_p\mathcal{Q}_p\bar{\Phi}_p. \quad (29)$$

- Dp in canonical ensemble & $D(p+4)$ in grand canonical ensemble (denoted as CG ensemble)

$$I_{CG} = \bar{\beta}E - S - \bar{\beta}V_{p+4}\mathcal{Q}_{p+4}\bar{\Phi}_{p+4}. \quad (30)$$

- Both charges are in grand canonical ensemble (denoted as GG ensemble)

$$I_{GG} = \bar{\beta}E - S - \bar{\beta}V_p\mathcal{Q}_p\bar{\Phi}_p - \bar{\beta}V_{p+4}\mathcal{Q}_{p+4}\bar{\Phi}_{p+4}. \quad (31)$$

Here, $\bar{\Phi}_p$ and $\bar{\Phi}_{p+4}$ are the potentials imposed on the boundary and we stick to the convention that the barred quantities are the ones on the boundary. Only at equilibrium, $\bar{\Phi}_p = \Phi_p$ and $\bar{\Phi}_{p+4} = \Phi_{p+4}$, and

$$I_{GC} = I_c + I_{b,p+4}, \quad I_{CG} = I_c + I_{b,p}, \quad I_{GG} = I_c. \quad (32)$$

It is easy to check that, for $\rho_b \rightarrow \infty$, (28) reduces to

$$E\Big|_{\rho_b \rightarrow \infty} = \frac{V_p^*V_4^*\Omega_{4-p}}{2\kappa^2}\left[(4-p)\rho_+^{3-p} + (2-p)\rho_-^{3-p} - (3-p)k\right] \quad (33)$$

the right hand side of which is exactly the ADM mass of the branes. We know that the free energy equals to its internal energy minus the temperature times the entropy, where the internal energy is the ADM mass for a gravitational system according to Bardeen et. al. [32]. So (27) and (33) means that we are indeed dealing with a system in canonical ensemble.

Now we justify that (27) (29) (30) and (31) are indeed the correct forms of free energy or grand potential, and the conjugate potentials defined in (20) and (22) are consistent. For this purpose, we will check that the equilibrium corresponds to the stationary point in various ensembles. First we take the derivative of I_{CC} with respect to $\bar{\rho}_+$ and set it to zero,

$$\frac{\partial I_{CC}}{\partial \bar{\rho}_+} = \frac{2\pi(3-p)V_{p+4}\Omega_{4-p}\bar{\rho}_+^{2-p}\bar{\rho}_b}{\kappa^2}f(\bar{\rho}_+, \tilde{\mathcal{Q}}_p, \tilde{\mathcal{Q}}_{p+4})\left[\bar{b} - b(\bar{\rho}_+, \tilde{\mathcal{Q}}_p, \tilde{\mathcal{Q}}_{p+4})\right] = 0, \quad (34)$$

where

$$\begin{aligned}
\bar{b} &= \frac{\bar{\beta}}{4\pi\bar{\rho}_b}, \\
b(\bar{\rho}_+, \tilde{Q}_p, \tilde{Q}_{p+4}) &= \frac{1}{3-p}(1-\bar{\Delta}_+)^{\frac{1}{2}} \left(\frac{\bar{\Delta}_+}{\bar{\Delta}_-}\right)^{\frac{1}{2}} \left(1-\frac{\bar{\Delta}_+}{\bar{\Delta}_-}\right)^{\frac{p-2}{3-p}} \left(1-\frac{\bar{\Delta}_+}{\bar{\Delta}_*}\right)^{\frac{1}{2}}, \\
f(\bar{\rho}_+, \tilde{Q}_p, \tilde{Q}_{p+4}) &= \frac{1}{2\bar{\Delta}_+^{1/2}\bar{\Delta}_-^{3/2}(1-\bar{\Delta}_+)} \left[(3-p)\bar{\Delta}_-(\bar{\Delta}_- - \bar{\Delta}_+) + 2(\bar{\Delta}_+ + \bar{\Delta}_- - 2\bar{\Delta}_+\bar{\Delta}_-) \right. \\
&\quad \left. + (3-p)\frac{\bar{\Delta}_-(\bar{\Delta}_- - \bar{\Delta}_+)(\bar{\Delta}_+ + \bar{\Delta}_- - 2\bar{\Delta}_+\bar{\Delta}_-)}{\bar{\Delta}_*\bar{\Delta}_+ + \bar{\Delta}_*\bar{\Delta}_- - 2\bar{\Delta}_+\bar{\Delta}_-} \right]. \tag{35}
\end{aligned}$$

The solution to (34) is the stationary point of the action, which is supposed to correspond to the equilibrium state, and is thus expected to give the equation of state (19). Since $\bar{\Delta}_+ < \bar{\Delta}_- \leq \bar{\Delta}_* \leq 1$, which can be seen from (9), the function f defined in the last equation of (35) is positive definite. This means the expression in the square brackets of (34) must vanish, which recovers the equation of state (19) exactly. This justifies our claim that I_{CC} is the correct form of free energy.

Next we take the derivative of I_{GC} with respect to Q_p and again set it to zero,

$$\begin{aligned}
\frac{\partial I_{GC}}{\partial Q_p} &= -\frac{\bar{\beta}V_p}{\sqrt{2\kappa e^{a_p\bar{\phi}/2}}} \left\{ \bar{\Phi} - \Phi(\bar{\rho}_+, \tilde{Q}_p, \tilde{Q}_{p+4}) \left[1 + \right. \right. \\
&\quad \left. \left. \left(1 - \frac{b(\bar{\rho}_+, \tilde{Q}_p, \tilde{Q}_{p+4})}{\bar{b}} \right) \frac{\bar{\Delta}_*(\bar{\Delta}_- - \bar{\Delta}_+)}{\bar{\Delta}_*\bar{\Delta}_+ + \bar{\Delta}_*\bar{\Delta}_- - 2\bar{\Delta}_+\bar{\Delta}_-} \right] \right\} \\
&= -\frac{\bar{\beta}V_p}{\sqrt{2\kappa e^{a_p\bar{\phi}/2}}} \left[\bar{\Phi} - \Phi(\bar{\rho}_+, \tilde{Q}_p, \tilde{Q}_{p+4}) \right] \\
&= 0 \tag{36}
\end{aligned}$$

where

$$\begin{aligned}
\bar{\Phi} &= \sqrt{2\kappa e^{a_p\bar{\phi}/2}} \bar{\Phi}_p, \\
\Phi(\bar{\rho}_+, \tilde{Q}_p, \tilde{Q}_{p+4}) &= \left(\frac{\bar{\Delta}_+}{\bar{\Delta}_-}\right)^{1/2} \left(\frac{\bar{\Delta}_* - \bar{\Delta}_-}{\bar{\Delta}_* - \bar{\Delta}_+}\right)^{1/2}. \tag{37}
\end{aligned}$$

In getting the first equality in (36), we have used the expression for \tilde{Q}_p in (14), and in the second equality, we have used the fact that $\bar{b} = b(\bar{\rho}_+, \tilde{Q}_p, \tilde{Q}_{p+4})$ in equilibrium state. The last equality in (36) just recovers the first equation in (22) where it is merely a definition. This proves the validity of that definition. Similarly, we calculate the derivative of I_{CG} with respect to Q_{p+4} ,

$$\begin{aligned}
\frac{\partial I_{CG}}{\partial Q_{p+4}} &= -\frac{\bar{\beta}V_p}{\sqrt{2\kappa e^{a_{p+4}\bar{\phi}/2}}} \left\{ \bar{\varphi} - \varphi(\bar{\rho}_+, \tilde{Q}_{p+4}) \left[1 - \left(1 - \frac{b(\bar{\rho}_+, \tilde{Q}_p, \tilde{Q}_{p+4})}{\bar{b}} \right) \times \right. \right. \\
&\quad \left. \left. \left(\frac{2}{3-p} \frac{1}{\bar{\Delta}_-} + \frac{\bar{\Delta}_- - \bar{\Delta}_+}{\bar{\Delta}_*\bar{\Delta}_+ + \bar{\Delta}_*\bar{\Delta}_- - 2\bar{\Delta}_+\bar{\Delta}_-} \right) \right] \right\} \\
&= -\frac{\bar{\beta}V_p}{\sqrt{2\kappa e^{a_{p+4}\bar{\phi}/2}}} \left[\bar{\varphi} - \varphi(\bar{\rho}_+, \tilde{Q}_{p+4}) \right], \tag{38}
\end{aligned}$$

where

$$\begin{aligned}\bar{\varphi} &= \sqrt{2\kappa}e^{a_{p+4}\bar{\phi}/2}\bar{\Phi}_{p+4}, \\ \varphi(\bar{\rho}_+, \tilde{\mathcal{Q}}_{p+4}) &= \left(\frac{\bar{\Delta}_+}{\bar{\Delta}_-}\right)^{1/2} \left(\frac{1-\bar{\Delta}_-}{1-\bar{\Delta}_+}\right)^{1/2}.\end{aligned}\quad (39)$$

Again in getting this result we have used (14) and the equation of state. Setting this derivative to zero would give exactly the second expression in (22). In the same fashion, if we partially differentiate I_{GG} with respect to $\bar{\rho}_+$, \mathcal{Q}_p and \mathcal{Q}_{p+4} , we would obtain all the three equations in (19) and (22).

For future simplifications in the computation, we define some reduced quantities in the following. The reduced action in the CC ensemble is defined as

$$\begin{aligned}\tilde{I}_{CC} &\equiv \frac{\kappa^2 I_{CC}}{2\pi\bar{\rho}_b^{4-p}V_{p+4}\Omega_{4-p}} \\ &= -\bar{b} \left[2 \left(\frac{\bar{\Delta}_+}{\bar{\Delta}_-}\right)^{1/2} + (3-p)(\bar{\Delta}_+\bar{\Delta}_-)^{1/2} \left(1 + \frac{1}{\bar{\Delta}_*}\right) + 2p - 8 \right] \\ &\quad - (1-\bar{\Delta}_+)^{1/2} \left(1 - \frac{\bar{\Delta}_+}{\bar{\Delta}_-}\right)^{\frac{1}{3-p}} \left(1 - \frac{\bar{\Delta}_+}{\bar{\Delta}_*}\right)^{1/2}.\end{aligned}\quad (40)$$

Other reduced quantities can be defined as follows,

$$x \equiv \left(\frac{\bar{\rho}_+}{\bar{\rho}_b}\right)^{3-p} < 1, \quad Q \equiv \tilde{\mathcal{Q}}_p < 1, \quad q \equiv \left(\frac{\tilde{\mathcal{Q}}_{p+4}}{\bar{\rho}_b}\right)^{3-p} < x.\quad (41)$$

Accordingly, in the reduced variables, $\bar{\Delta}_{+,-,*}$ and the other reduced actions can be expressed as

$$\begin{aligned}\bar{\Delta}_+ &= 1 - x, \\ \bar{\Delta}_- &= 1 - \frac{q^2}{x}, \\ \bar{\Delta}_* &= \frac{\bar{\Delta}_+ + \bar{\Delta}_- + \sqrt{(\bar{\Delta}_- - \bar{\Delta}_+)^2 + 4Q^2\bar{\Delta}_+\bar{\Delta}_-}}{2(1-Q^2)},\end{aligned}\quad (42)$$

and

$$\begin{aligned}\tilde{I}_{GC} &= \tilde{I}_{CC} - (3-p)\bar{b}Q\bar{\Phi}, \\ \tilde{I}_{CG} &= \tilde{I}_{CC} - (3-p)\bar{b}q\bar{\varphi}, \\ \tilde{I}_{GG} &= \tilde{I}_{CC} - (3-p)\bar{b}Q\bar{\Phi} - (3-p)\bar{b}q\bar{\varphi}.\end{aligned}\quad (43)$$

Notice that $\bar{\Delta}_+$ only depends on x , and $\bar{\Delta}_-$ depends on both q and x , while $\bar{\Delta}_*$ depends on all three variables x , q and Q . With (40) and (43), we find again the equations of equilibrium state

corresponding to (34), (36) and (38), in reduced quantities,

$$\begin{aligned}
\frac{\partial \tilde{I}_{GC}}{\partial Q} &= -(3-p)\bar{b} \left\{ \bar{\Phi} - \Phi(x, Q, q) \left[1 + \left(1 - \frac{b(x, Q, q)}{\bar{b}} \right) \frac{\bar{\Delta}_*(\bar{\Delta}_- - \bar{\Delta}_+)}{\bar{\Delta}_*\bar{\Delta}_+ + \bar{\Delta}_*\bar{\Delta}_- - 2\bar{\Delta}_+\bar{\Delta}_-} \right] \right\}, \\
\frac{\partial \tilde{I}_{CG}}{\partial q} &= -(3-p)\bar{b} \left\{ \bar{\varphi} - \varphi(x, q) \left[1 - \left(1 - \frac{b(x, Q, q)}{\bar{b}} \right) \left(\frac{2}{3-p} \frac{1}{\bar{\Delta}_-} + \frac{\bar{\Delta}_- - \bar{\Delta}_+}{\bar{\Delta}_*\bar{\Delta}_+ + \bar{\Delta}_*\bar{\Delta}_- - 2\bar{\Delta}_+\bar{\Delta}_-} \right) \right] \right\}, \\
\frac{\partial \tilde{I}_{CC}}{\partial x} &= f(x, Q, q) [\bar{b} - b(x, Q, q)],
\end{aligned} \tag{44}$$

where the functions f , b , Φ and φ have been defined in (35), (37) and (39). Notice that from (9), we find $0 < \Phi < 1$ and $0 < \varphi < 1$ for nonzero p - and $(p+4)$ -brane charges when the horizon is not coincident with the boundary.

3 Thermodynamics in different ensembles

Note that when $Q = 0$, the whole system becomes a $D(p+4)$ -brane system, and the various phase structures of this system have already been thoroughly analyzed in [5, 33]. Thus, in the following calculations, we will always assume that $Q > 0$ ($\bar{\Phi} > 0$). Nevertheless, we will still compare our results with the $Q = 0$ case for consistency check or revealing the different traits in the presence of Dp -branes.

3.1 Overview of the behaviors of $b(x)$

Before performing concrete analyses in specific ensembles, we first examine a few typical behaviors of the function $b(x, Q, q)$, which are useful in our later exploration.

In the following discussions of the phase structures in these ensembles, the key problems to be solved are finding out the stationary points of thermodynamic potentials and which one is stable. That is, we need to solve the following equations,

$$\begin{aligned}
b(x, Q, q) &= \bar{b}, \\
\Phi(x, Q, q) &= \bar{\Phi}, \\
\varphi(x, q) &= \bar{\varphi},
\end{aligned} \tag{45}$$

and then determine whether the solution(s) to these equations is the minimum point of those thermodynamic potentials. In the CC ensemble, we need the first equation only. In the CG ensemble, we need the first and the third ones and in the GC ensemble, we need the first and the second ones. In GG ensemble, we need all the three equations. To discuss the stabilities of the system at the stationary points, one needs to discuss the positivity of the Hessian matrix of the thermodynamic potential with respect to these variables. In CC ensemble, the Hessian involves only one variable x . Similar to the grand canonical ensemble for R-N black hole discussed by [4], in GC or CG the Hessian involves two variables and in GG ensemble, it involves three variables. However, there is a simplified

version of the discussion in which the potentials conjugate to the charges are supposed to be already in equilibrium and are fixed at the classical solution as in the second and the third equations in (45), and the Hessian only involves one variable x . This kind of analysis is also widely used, for example in [6, 7, 33, 13] and for one-charge black brane it was proved to be the same as the two variable analysis [33]. Here, we would adopt the simplified version in our analysis, i.e. the second and third equations in (45) have already been satisfied[33, 13], and Q and q can be solved and be substituted in the first equation. Thus, the only problem left is to solve the first equation where b is a function of just one variable x , that is,

$$b(x) \Big|_{\Phi=\bar{\Phi} \text{ or/and } \varphi=\bar{\varphi}} = \bar{b}, \tag{46}$$

for corresponding ensembles. In that case, the local minimum condition of the thermodynamical potential would simply be

$$\frac{d^2 I}{dx^2} > 0. \tag{47}$$

In equation (46), \bar{b} is the inverse temperature on the boundary which is assumed to be a constant input parameter. Hence finding out the solution is equivalent to finding out the intersection points of curve $b = b(x)$ and the horizontal line $b = \bar{b}$. On the other hand, we will demonstrate that

$$\frac{d^2 I}{dx^2} \sim -\frac{db}{dx}, \tag{48}$$

which means the local minimum point is the intersection point where $\frac{db}{dx}$ (the slope) is negative.

We will see in the GG ensemble, that there are only two kinds of curves for $b(x)$ which are listed in Figure 1. One can see that, in the first graph of Figure 1, although there is an intersection point

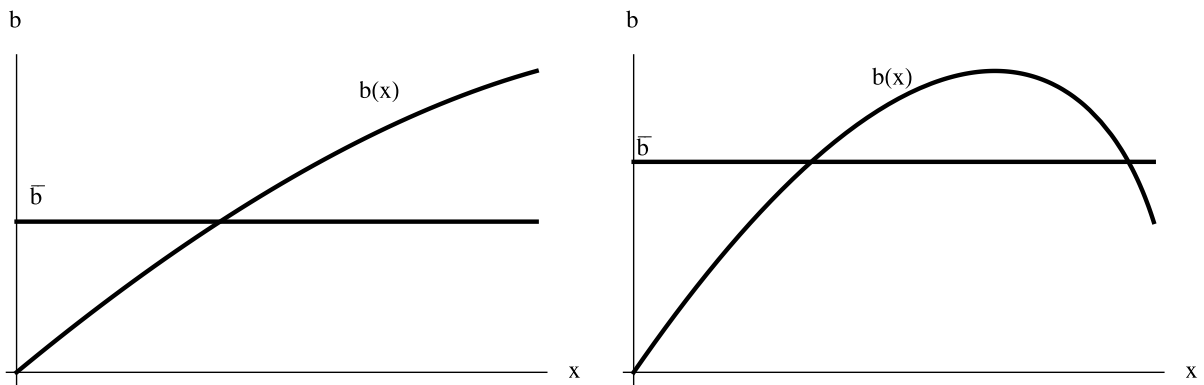


Figure 1: Typical behaviors of $b(x)$ in GG ensembles as well as in some cases in GC and CG ensemble.

of the two curves, it is not a minimum of grand potential since the slope at that point is positive. We therefore conclude that there is no stable black brane phase for any \bar{b} given that $b(x)$ increases monotonically. In this case, since the hot flat space can have the same boundary condition with the

brane, the only stable phase should be the hot flat space. However, in the second graph, for \bar{b} within some range, there could be two intersection points, where the slope is negative at the one with larger x . Thus we conclude that there will be a locally stable black brane phase for \bar{b} within that range, i.e., the brane configuration with larger horizon is locally stable. To find out whether it is a globally stable phase, we have to compare the grand potential at this point with the one for the hot flat space, i.e. the one at $x = 0$. If the grand potential at this point is a global minimum it would be the real stable phase, otherwise it is merely a locally stable one. In this section, we only concentrate on locally stable phases.

In the GC ensemble, there will be much richer phase structures. For $p = 2$ (D2-D6 system), the possible curves of $b(x)$ are the same as the ones for the GG ensemble, and therefore we do not need to reanalyse them. For $p = 1$ case (D1-D5 system), there will be one more possible shape besides the two appearing in Figure 1. This new curve monotonically decreases as shown in Figure 2. Thus, if

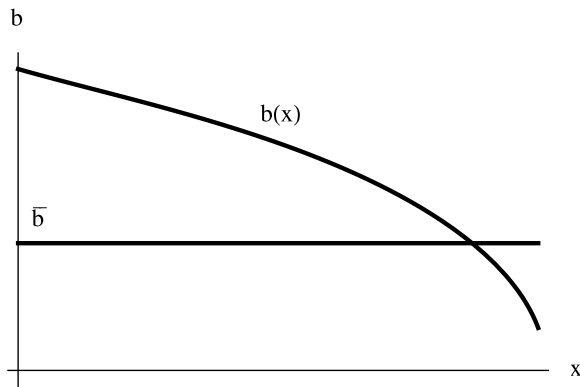


Figure 2: A typical curve in GC ensemble for $p = 1$ besides those in Figure 1.

the constant \bar{b} line intersects with $b(x)$ curve at some point, this point must correspond to a globally stable black brane phase. If $p = 0$ (D0-D4 system), there are three cases as shown in Figure 3. The third one as shown in Figure 3(c) is similar to Figure 2 with decreasing $b(x)$. In Figure 3(a), if $\bar{b} = \bar{b}_1$ ($\bar{b} > b_{GC}(x_{max})$), there is only one intersection point at which the state is stable, whereas if $\bar{b} = \bar{b}_2$ ($\bar{b} < b_{GC}(x_{max})$), there will be two intersection points and only the one with smaller x is locally stable. For the second graph, there are more possibilities. We can see that if $\bar{b} = \bar{b}_1 > b_{max}$ or $\bar{b} = \bar{b}_3 < b_{min}$, where b_{min} and b_{max} are the local minimum and local maximum of $b(x)$ as shown in the graph, there is only one intersection point and it is a stable black brane phase. Yet for $\bar{b} = \bar{b}_2$ with $b_{min} < \bar{b}_2 < b_{max}$, there can be three intersection points. Denoting these three points as x_1, x_2 and x_3 with $x_1 < x_2 < x_3$, one can see that the point with $x = x_2$ is apparently unstable for its positive slope while the other two are both locally stable. As regards these two locally stable phases, the one with higher free energy will eventually transit to the other phase. It can be shown that there exists some value of \bar{b} between b_{min} and b_{max} , at which the two locally stable phases have equal thermodynamic potentials but different entropies, which indicates a first order phase transition, i.e. the van der Waals-like phase

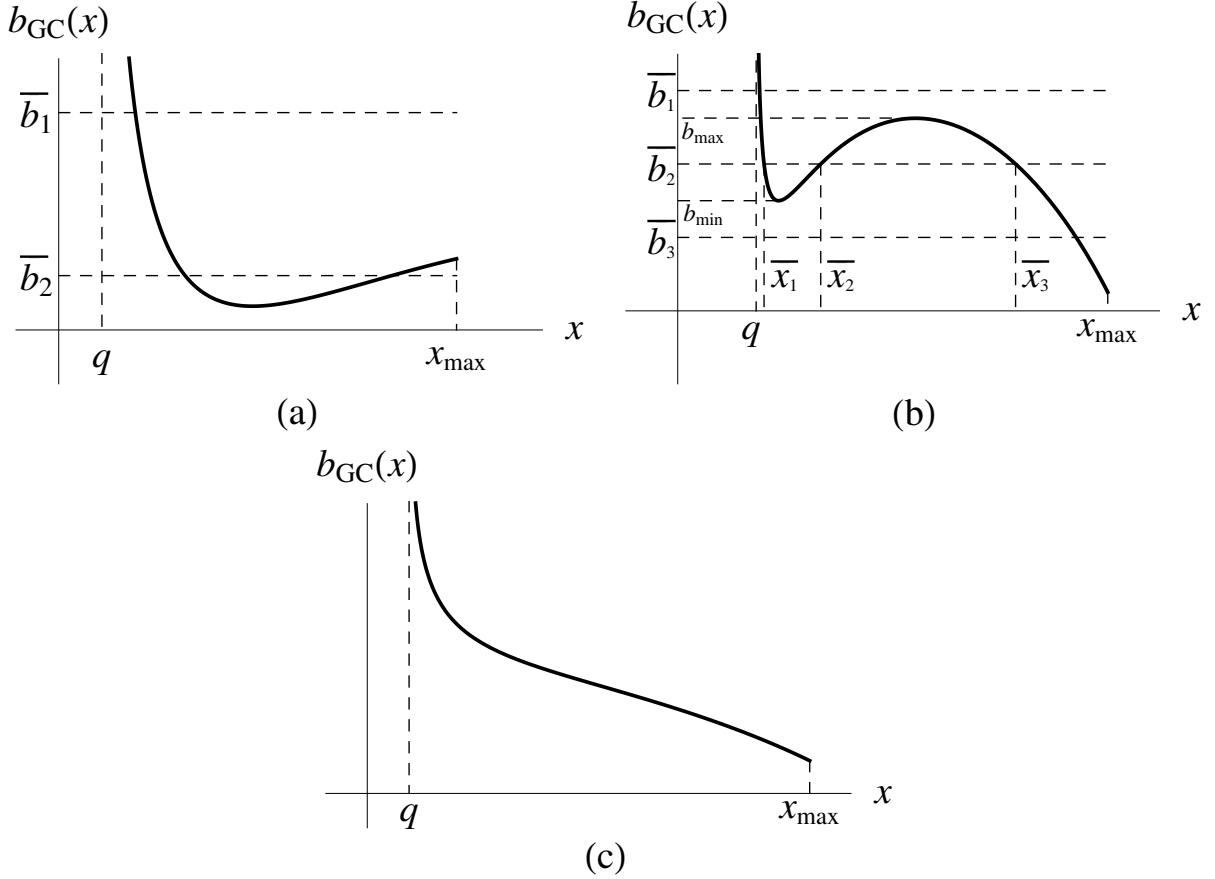


Figure 3: Typical $b(x)$ behaviors in GC ensemble for $p = 0$

transition. The second graph in Figure 3 is just a typical case of this kind which is similar to the one-charge black brane. In two-charge case $b(x_{max})$ does not reach zero, so there can be possibilities that $b(x_{max}) > b_{min}$. We will discuss this case in section 3.3.

In the CG ensemble, all three possible $b(x)$ curves in Figure 3 also appear here. As argued in [29], in the CC ensemble, the delocalized Dp -branes and the $D(p + 4)$ -branes are equipotent in the sense that exchanging the two kinds of brane charges would yield similar phase structures. This reveals some symmetry under exchange of the boundary conditions that we have imposed on these two kinds of branes. The GC and CG ensemble are just related by an exchange of the boundary conditions on these two kinds of branes and we will see later that the phase structures of these two ensembles are really related in this way.

Now having found all the patterns of the $b(x)$ curves and the locally stable phase in each case qualitatively, we need to be specific in each ensemble to find out in what ranges of the parameter Q (or $\bar{\Phi}$) and q (or $\bar{\varphi}$) one can have a certain pattern of $b(x)$. Then, we would know the possible state of the system given any pair of Q (or $\bar{\Phi}$) and q (or $\bar{\varphi}$). The following subsections are devoted to this problem.

The CC ensemble (especially when $p = 1$) has already been explored by Lu et al. in [29], and we have gathered some results in Appendix A including some facts not given in [29]. Interested readers are referred to their paper for more details. In the following subsections we will focus on the other three kinds of ensembles.

3.2 GG ensemble

As stated in the previous section, we adopt the one variable analysis as an embryo attempt to find out the thermodynamical structure. We need to solve Q and q in terms of x and the corresponding electric potentials on the boundary ($\bar{\Phi}$ and $\bar{\varphi}$), from the two electromagnetic equilibrium equations, i.e. the second and the third equations in (45), using (37) and (39). Since the Q and q dependence comes from $\bar{\Delta}_-$ and $\bar{\Delta}_*$, it is convenient to first express $\bar{\Delta}_-$ and $\bar{\Delta}_*$ in terms of x , $\bar{\Phi}$ and $\bar{\varphi}$,

$$\bar{\Delta}_- = \frac{\bar{\Delta}_+}{\xi}, \quad \bar{\Delta}_* = \bar{\Delta}_+ \frac{1 - \bar{\Phi}^2}{\xi - \bar{\Phi}^2}, \quad (49)$$

where $\xi = 1 - (1 - \bar{\varphi}^2)x < 1$. Then the charges can easily be obtained,

$$q = \frac{x\bar{\varphi}}{\xi^{1/2}}, \quad Q = \frac{\bar{\Phi}(1 - \xi)}{(1 - \bar{\Phi}^2)\xi^{1/2}}. \quad (50)$$

The reduced action which is proportional to the grand potential can then be obtained in terms of x , $\bar{\varphi}$ and $\bar{\Phi}$,

$$\tilde{I}_{GG} = 2(4 - p)(1 - \sqrt{\xi})[\bar{b} - b_0(x)] \quad (51)$$

where

$$b_0(x) \equiv \frac{1 + \xi^{1/2}}{2(4 - p)} \left(\frac{x}{1 - \bar{\Phi}^2} \right)^{1/2} (1 - \xi)^{\frac{1-p}{2(3-p)}}. \quad (52)$$

We have mentioned in (9) that $\rho_+^{3-p} > \rho_-^{3-p} > k$. This inequality can be rewritten in terms of $\bar{\Delta}_+$, $\bar{\Delta}_-$ and $\bar{\Delta}_*$,

$$\bar{\Delta}_+ < \bar{\Delta}_-, \quad \bar{\Delta}_- < \bar{\Delta}_*. \quad (53)$$

The first relation in (53) is guaranteed by the first equality of (49). The second relation holds only for

$$x < \frac{1 - \bar{\Phi}^2}{1 - \bar{\varphi}^2}. \quad (54)$$

So, we have a restriction on x ,

$$0 < x < x_{max} = \min \left\{ 1, \frac{1 - \bar{\Phi}^2}{1 - \bar{\varphi}^2} \right\}. \quad (55)$$

For $\bar{\Phi} < \bar{\varphi}$, $x_{max} = 1$ which means the horizon should be inside the boundary. For $\bar{\Phi} > \bar{\varphi}$, the condition is the requirement of $Q < 1$. This limit should not be reached since otherwise Δ_* would blow up and

the size of the time direction and some space dimensions would shrink to zero. In fact, before it shrinks to string scale, the quantum effects should be large, and the supergravity approximation is invalid. Thus, if at x_{max} the system has lower grand potential than at the local minimum, we will regard the system as unstable, since either the horizon tends to the boundary or the supergravity approximation is not applicable. At $x = 0$, the charges tends to zero, the system reduce to the “hot flat space”.

Next, we need to find out the stationary point by setting

$$0 = \left. \frac{\partial \tilde{I}_{GG}(x, \bar{\Phi}, \bar{\varphi})}{\partial x} \right|_{\bar{\Phi}, \bar{\varphi}} = f_{GG}(x) [\bar{b} - b_{GG}(x)], \quad (56)$$

where

$$\begin{aligned} b_{GG}(x) &= \frac{1}{3-p} \left(\frac{x\xi}{1-\bar{\Phi}^2} \right)^{1/2} (1-\xi)^{-\frac{1-p}{2(3-p)}}, \\ f_{GG}(x) &= (4-p) \frac{1-\xi}{x\xi^{1/2}} > 0. \end{aligned} \quad (57)$$

Equation (56) again reduces to the familiar one,

$$\bar{b} = b_{GG}(x). \quad (58)$$

Notice that at $x = 0$, b_{GG} is always zero. So b_{GG} should be increasing near $x = 0$ due to the fact that $b_{GG} \geq 0$, i.e. $db_{GG}(x)/dx \geq 0$ at $x = 0$. Finally the local stability condition is effectively

$$\frac{d^2 \tilde{I}_{GG}(\bar{x})}{dx^2} \sim -\frac{db_{GG}(\bar{x})}{dx} > 0, \quad (59)$$

where \bar{x} is the solution to equation (58). The derivative of b_{GG} can be evaluated,

$$\frac{db_{GG}}{dx} = \frac{b_{GG}}{2(3-p)x\xi} [2 - (5-p)(1-\bar{\varphi}^2)x]. \quad (60)$$

Thus, the condition (59) is equivalent to

$$2 - (5-p)(1-\bar{\varphi}^2)\bar{x} < 0, \quad (61)$$

which is exactly the same condition as for black $(p+4)$ -brane without p -brane charge, i.e. the (35) in [33], except that now the solution \bar{x} depends on a new parameter $\bar{\Phi}$.

From (60), we see that there is a turning point

$$x_0 = \frac{2}{5-p} \frac{1}{1-\bar{\varphi}^2}$$

where $b_{GG}(x)$ increases for $x < x_0$ and decreases for $x > x_0$. Therefore, if $x_{max} < x_0$, $b_{GG}(x)$ will be a monotonically increasing function for $x \in (0, x_{max})$, otherwise it will have a maximum at $x = x_0$. For the former case (referred to as *case A*), the curve of b_{GG} looks like the one in the first graph of

Figure 1, while for the latter case (referred to as *case B*) it looks like the curve in the second graph, just as we stated in the previous section.

We then need to figure out the condition for $\bar{\Phi}$ and $\bar{\varphi}$ in each case. We start by requiring $x_0 > x_{max}$, i.e.,

$$\frac{2}{(5-p)(1-\bar{\varphi}^2)} > \min \left\{ 1, \frac{1-\bar{\Phi}^2}{1-\bar{\varphi}^2} \right\}. \quad (62)$$

which would give

$$\bar{\Phi} > \sqrt{\frac{3-p}{5-p}} \quad \text{or} \quad \bar{\varphi} > \sqrt{\frac{3-p}{5-p}}. \quad (63)$$

That means that for $\bar{\Phi}$ and $\bar{\varphi}$ satisfying (63), case A is applied and the system cannot have a stable black brane phase. On the contrary, if

$$\bar{\Phi} < \sqrt{\frac{3-p}{5-p}} \quad \text{and} \quad \bar{\varphi} < \sqrt{\frac{3-p}{5-p}}, \quad (64)$$

$b_{GG}(x)$ will look like the curve in Figure 4. One can see that if $b_1 > \bar{b} > b_2$, there can be a locally

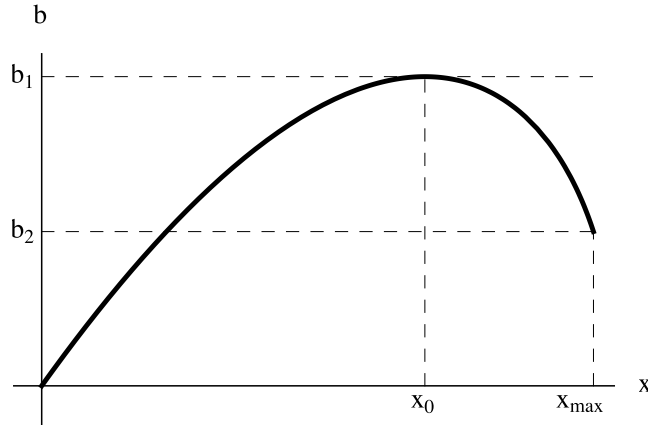


Figure 4: b_{GG} for $x_0 < x_{max}$. For $\bar{\Phi} < \bar{\varphi}$, $x_{max} = 1$, otherwise $x_{max} = \frac{1-\bar{\Phi}^2}{1-\bar{\varphi}^2}$.

stable black brane phase and its horizon radius is between x_0 and x_{max} , where b_1 and b_2 are defined by

$$\begin{aligned} b_1 &= b_{GG}(x_0) = \frac{2^{\frac{1}{3-p}} (5-p)^{-\frac{5-p}{2(3-p)}}}{\sqrt{(3-p)(1-\bar{\Phi}^2)(1-\bar{\varphi}^2)}}, \\ b_2 &= b_{GG}(x_{max}) = \begin{cases} \frac{\bar{\varphi}(1-\bar{\varphi}^2)^{\frac{1-p}{2(3-p)}}}{(3-p)\sqrt{1-\bar{\Phi}^2}}, & \text{for } \bar{\Phi} < \bar{\varphi}; \\ \frac{\bar{\Phi}(1-\bar{\Phi}^2)^{\frac{1-p}{2(3-p)}}}{(3-p)\sqrt{1-\bar{\varphi}^2}}, & \text{for } \bar{\varphi} < \bar{\Phi}. \end{cases} \end{aligned} \quad (65)$$

For \bar{b} not in this range, there will be no stable black brane phase.

Combining the arguments above, we would have the diagram shown in Figure 5 which gives a more explicit view of the answer to the previous question. In this figure, the two constants are

$$\bar{\Phi}_0 = \bar{\varphi}_0 = \sqrt{\frac{3-p}{5-p}}. \quad (66)$$

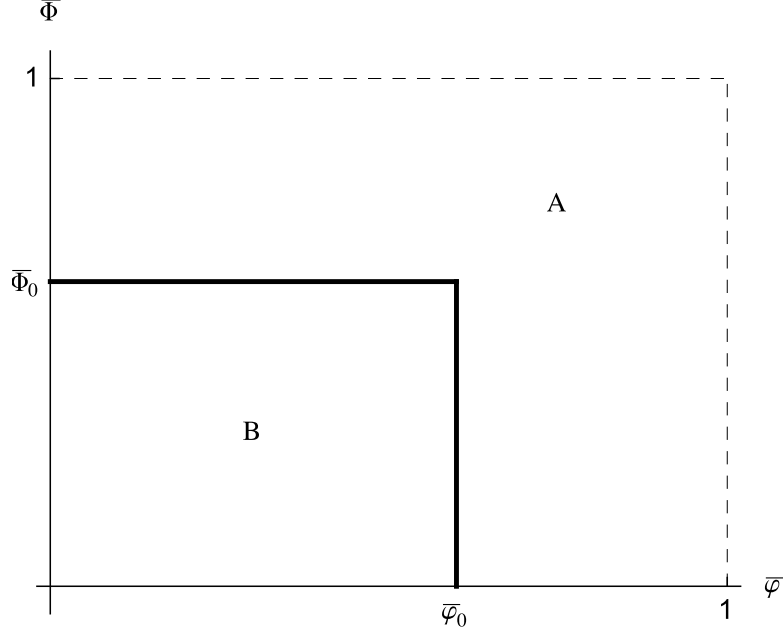


Figure 5: Parameter plane in GG ensemble

Since the charges are not conserved in grand canonical ensemble, the hot flat space can be a possible phase. In region A, at very low temperature with $\bar{b} > b_2$ where $\partial I_{GG}/\partial x > 0$, the grand potential is a monotonically increasing function of x as shown in Figure 6(a) (we will use the subfigure labels to denote different cases). Since the hot flat space has $x = 0$, the final stable phase should be the hot flat space. If $\bar{b} < b_2$, there can be two cases which are shown in (b) and (c) in Figure 6. In the first case (b), which has lower temperature than (c), the minimum of the action is still at $x = 0$ which corresponds to the hot flat space. For case (c) which has higher temperature, the global minimum of the I_{GG} is at the boundary x_{max} which means that the hot flat space is not a global minimum of the grand potential and hence is unstable, and the horizon of the black brane tends to expand to the boundary. This means that there is no stable phase in this region. We can find out the condition for this case by solving the inequality $I_{GG}(x_{max}) < 0$ which gives

$$\bar{b} < b_{\text{unstable}} = \begin{cases} \frac{(1-\bar{\Phi})^{-\frac{1-p}{2(3-p)}}}{2(4-p)\sqrt{1-\bar{\varphi}^2}}, & \text{for } \bar{\Phi} > \bar{\varphi} \\ \frac{(1-\bar{\varphi})^{-\frac{1-p}{2(3-p)}}}{2(4-p)\sqrt{1-\bar{\Phi}^2}}, & \text{for } \bar{\varphi} > \bar{\Phi} \end{cases} \quad (67)$$

So for temperatures larger than $1/b_{\text{unstable}}$ the system is unstable. We do not know what really happens at this high temperature. Below this temperature, only hot flat space is the stable phase. Region B, where $\max(\bar{\Phi}, \bar{\varphi}) < \sqrt{\frac{3-p}{5-p}}$, has more cases to be considered. First, for very low temperatures, similar to case A, when there is no solution for (56), I_{GG} behaves as Figure 6(a) and the stable phase is the hot flat space. For higher temperatures when (56) has two solutions, i.e. $b_2 < \bar{b} < b_1$, I_{GG} has two stationary points, one unstable and the other locally stable. The possible behaviors of I_{GG} are shown in (d) and (e) in Figure 6. For case (d) which has lower temperature, the hot flat space at $x = 0$ has the lowest grand potential, and hence is the stable phase. At higher temperatures such that the system corresponds to graph (e), the grand potential at the locally stable point is negative and becomes the global minimum. So in this case the final stable phase is the black brane. For certain $\bar{\Phi}$ and $\bar{\varphi}$, case (e) can not happen. We can find out the condition for (e) to happen by looking at $I_{GG}(\bar{x}) = 0$. We put the detailed analysis in Appendix B and only state the results here. Firstly, when

$$\max(\bar{\Phi}, \bar{\varphi}) > \frac{3-p}{5-p}, \quad (68)$$

for $\bar{b} > b_2$, $I_{GG}(\bar{x})$ is always positive which corresponds to graph (d). Under this circumstance, the cases corresponding to graph (e) does not happen. With such $\bar{\Phi}$ and $\bar{\varphi}$, when $\bar{b} \in (b_{\text{unstable}}, b_2)$, there is only one solution to (56), which also corresponds to (b) in Figure 6. Hot flat space is then the global minimum as in case A. For higher temperatures such that $\bar{b} < b_{\text{unstable}}$, graph (c) also appears and the system is unstable. Secondly, when

$$\max(\bar{\Phi}, \bar{\varphi}) < \frac{3-p}{5-p}, \quad (69)$$

there is a temperature $T_0 \in (1/b_1, 1/b_2)$ at which the locally stable point is at $\bar{x}_0(\bar{\varphi}) \equiv \frac{4(4-p)}{(5-p)^2(1-\bar{\varphi}^2)}$. If the temperature is lower than T_0 such that at the locally stable point $\bar{x} < \bar{x}_0(\bar{\varphi})$, I_{GG} is positive (case (d)) and the hot flat space is the globally stable phase. Only for temperature higher than T_0 , when the locally stable point $\bar{x} > \bar{x}_0(\bar{\varphi})$, the black brane has a negative grand potential, which corresponds to graph (e) in Figure 6, and black brane is the final globally stable phase. For much higher temperature such that $\bar{b} < b_2$, the case corresponding to graph (c) also happens, and the system is again unstable. So combined with case A, for all $\max(\bar{\Phi}, \bar{\varphi}) > \frac{3-p}{5-p}$, the black brane can not be the final stable phase and for low temperatures the hot flat space is the global minimum. Only when $\max(\bar{\Phi}, \bar{\varphi}) < \frac{3-p}{5-p}$, the black brane can be the final stable phase for certain temperature $T \in (T_0, 1/b_2)$.

As we stated in the previous section, from the conditions (63, 64, 65, 66), we see that the phase structure is symmetric under the exchange of the boundary conditions imposed on the two kinds of branes, i.e. exchanging $\bar{\Phi}$ and $\bar{\varphi}$. We will also find similar results in GC and CG ensemble.

3.3 GC ensemble

In this ensemble, the $D(p+4)$ -brane charge q is fixed, therefore we only need to use the equation

$$\Phi(x, Q) = \bar{\Phi} \quad (70)$$

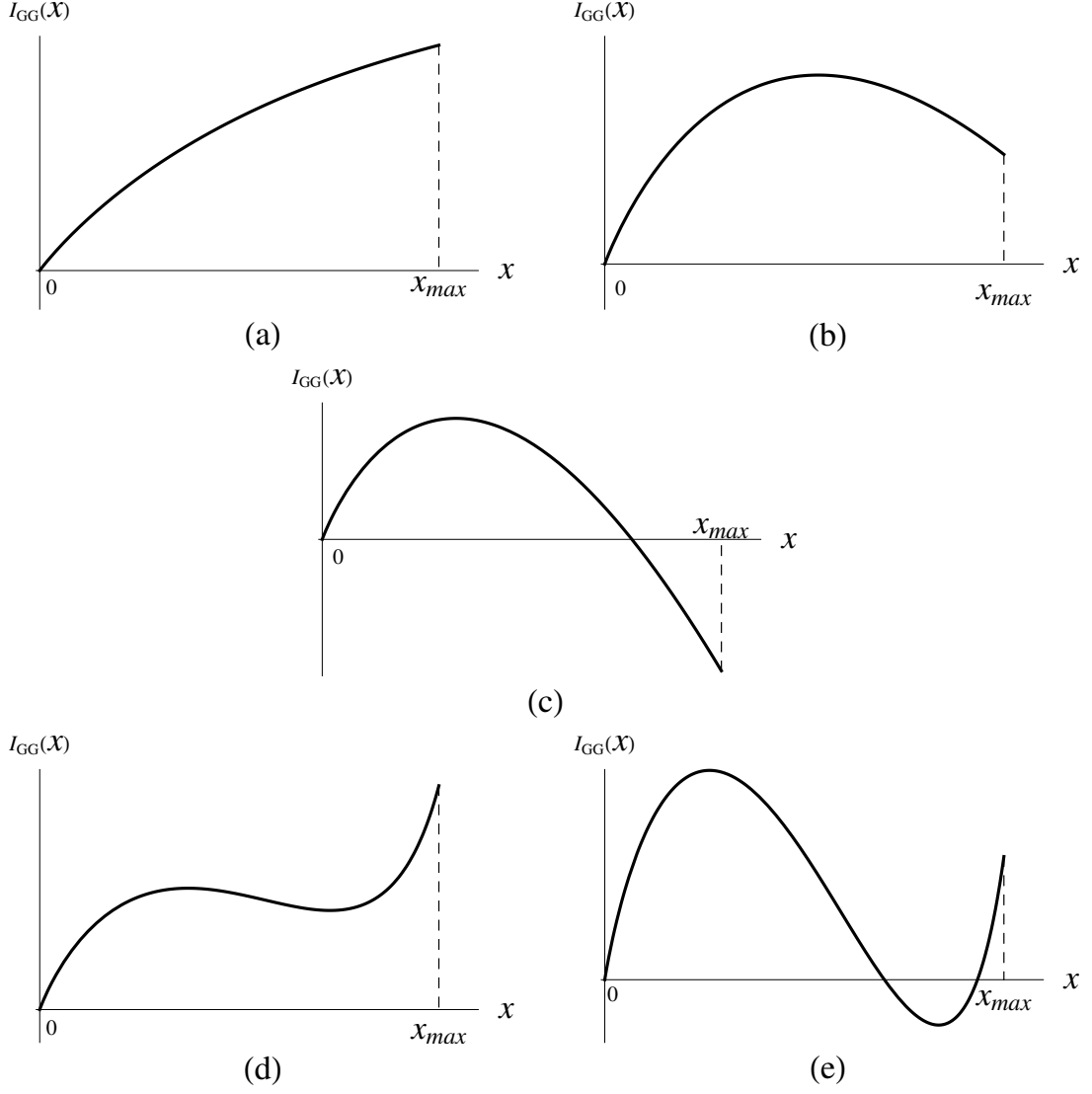


Figure 6: Typical $I_{GG}(x)$ behaviors in region A and B.

to get rid of the unfixed quantity Q . Since $\bar{\Phi}$ is fixed at the boundary, we can solve $\bar{\Delta}_*$ from this equation and then Q using (16),

$$\bar{\Delta}_* = \frac{\bar{\Delta}_+ \bar{\Delta}_- (1 - \bar{\Phi}^2)}{\bar{\Delta}_+ - \bar{\Delta}_- \bar{\Phi}^2}, \quad (71)$$

$$Q_{GC} = \frac{\bar{\Phi}(\bar{\Delta}_- - \bar{\Delta}_+)}{(1 - \bar{\Phi}^2)(\bar{\Delta}_+ \bar{\Delta}_-)^{1/2}}. \quad (72)$$

Using (71) and also requiring $\bar{\Delta}_+ < \bar{\Delta}_- < \bar{\Delta}_*$, we can find the domain of x ,

$$0 < q < x < x_{max} < 1, \quad (73)$$

where

$$x_{max} = \frac{1 - \bar{\Phi}^2 + \sqrt{(1 - \bar{\Phi}^2)^2 + 4q^2\bar{\Phi}^2}}{2}. \quad (74)$$

As in GG ensemble, when $x \rightarrow x_{max}$, Δ_* tends to infinity and could not be reached in supergravity approximation. At $x = q$, at which $\Delta_+ = \Delta_- = \Delta_*$ and $Q_{GC} = 0$, the system reduces to extremal $(p+4)$ -brane. However, the horizon of the extremal brane is singular and the quantum gravity effect must be non-negligible, and hence the Euclidean action method is not applicable. So if the global minimum of the reduced action is at the boundary $x = q$ or x_{max} , we do not know what the final stable state of the system is. So, we regard the system as unstable in our semi-classical description when the thermodynamical potential at $x = q$ or $x = x_{max}$ is lower than the local minimum value.

With relation (72), we can find the stationary point by solving equation

$$0 = \frac{d\tilde{I}_{GC}}{dx} = f_{GC}(x) [\bar{b} - b_{GC}(x)], \quad (75)$$

where

$$\begin{aligned} b_{GC}(x) &= b(x, Q_{GC}(x, q, \bar{\Phi}), q) = \frac{1}{3-p} \left(1 - \frac{\Delta_+}{\Delta_-}\right)^{\frac{p-1}{2(3-p)}} \sqrt{\frac{\Delta_+(1-\Delta_+)}{\Delta_-(1-\bar{\Phi}^2)}}, \\ f_{GC}(x) &= \frac{(3-p)\bar{\Delta}_-(\bar{\Delta}_- - \bar{\Delta}_+) + (5-p)(\bar{\Delta}_+ + \bar{\Delta}_- - 2\bar{\Delta}_+\bar{\Delta}_-)}{2\bar{\Delta}_+^{1/2}\bar{\Delta}_-^{3/2}(1-\bar{\Delta}_+)} > 0, \end{aligned} \quad (76)$$

which gives the equilibrium condition $\bar{b} = b_{GC}(x)$ as before. Assuming that $x = \bar{x}$ solves (75), the stability condition becomes

$$\frac{db_{GC}(\bar{x})}{dx} < 0. \quad (77)$$

Now we compute the derivative of b_{GC} ,

$$\left. \frac{db_{GC}}{dx} \right|_{q, \bar{\Phi}} = \frac{b_{GC}}{2x} \left(1 + \frac{(\bar{\Delta}_+ + \bar{\Delta}_- - 2\bar{\Delta}_+\bar{\Delta}_-)[2\bar{\Delta}_+ - (3-p)\bar{\Delta}_-]}{(3-p)\bar{\Delta}_+\bar{\Delta}_-(\bar{\Delta}_- - \bar{\Delta}_+)} \right). \quad (78)$$

We can see that in this expression, in the large parentheses, $\bar{\Delta}_*$ completely disappears, which means the equation is independent of $\bar{\Phi}$. For $\bar{\Phi} = 0$, i.e. D $(p+4)$ -brane without D p -brane charges, which is equivalent to setting $\bar{\Delta}_* = \bar{\Delta}_-$ in $b_{GC}(x)$, (78) would exactly recover the same equation for D $(p+4)$ -brane in canonical ensemble ((46) in [5]). This is also true even for $\bar{\Phi} \neq 0$ since it is independent of $\bar{\Phi}$, that is, (78) still gives the same condition to determine the signature of $\frac{db_{GC}}{dx}$ for $\bar{\Phi} = 0$, which was already given as in (47) of [5]. This means that the stationary point for $b_{GC}(x)$ is independent of $\bar{\Phi}$ and only depends on the charge q . To be specific, we rewrite (78) in terms of x and q ,

$$\frac{db_{GC}}{dx} = -g(x, q) \frac{b_{GC}}{x^4(1-x)(1-\frac{q^2}{x})(1-\frac{q^2}{x^2})}, \quad (79)$$

where

$$g(x, q) = \frac{5-p}{2}x^4 - \left(1 + \frac{7-p}{2}q^2\right)x^3 - \frac{3-3p}{2}q^2x^2 + q^2\left(2-p + \frac{9-3p}{2}q^2\right)x - (3-p)q^4. \quad (80)$$

Now (80) is exactly the function on the left hand side of (47) in [5] (there, a different parameter, the ‘‘co-dimension’’ \tilde{d} which is equal to $3-p$ in our case, is used). Therefore, condition (77) becomes a simpler one,

$$g(\bar{x}, q) > 0. \quad (81)$$

With (75) and (81) we can proceed with the phase structure analysis for different p .

First for $p = 2$ (D2-D6 system), notice that at $x = q$, $b_{GC} = 0$ which is the same as b_{GG} in GG ensemble at $x = 0$. As we have mentioned in section 3.1, there are only two possible shapes of $b_{GC}(x)$ which are similar to the cases in the GG ensemble (see Figure 1) with the only difference that the left end point of the $b_{GC}(x)$ is at $x = q$ here. Now we will find out the conditions for these two cases. From Figure 1 one can see that the difference of the two patterns is the sign of the slope of the curves at x_{max} . So one can conclude that there must be a transition line on the $\bar{\Phi} - q$ plane on which the $b_{GC}(x)$ curve has $db_{GC}(x)/dx = 0$ at x_{max} . Actually this is a universal feature for all p , so instead of solving it here for only $p = 2$ case we have done it for all p and put the tedious analytic computations in Appendix C. Here we just give the diagram in Figure 7 for $p = 2$, which has similar meaning as Figure 5. In region A, b_{GC} is a monotonically increasing function and there is no locally stable black brane phase. In region B, the $b_{GC}(x)$ curve is like Figure 4 and for $b_2 < \bar{b} < b_1$, there are two intersection points and the larger one is a locally stable black brane phase. The boundary between A and B on $q - \bar{\Phi}$ plane has the following form,

$$q = \frac{1 - \bar{\Phi}^2}{\bar{\Phi}(3 - 5\bar{\Phi}^2)} \sqrt{2(1 - \bar{\Phi}^2)(3\bar{\Phi}^2 - 1)}, \quad \frac{1}{\sqrt{3}} < \bar{\Phi} < \frac{1}{\sqrt{2}}. \quad (82)$$

The locally stable state may not be a global minimum of the reduced action because at the boundary $x = q$ the reduced action may have smaller value. To find out the condition that the local minimum can not be the global minimum for $b_2 < \bar{b} < b_1$ one can look at the critical case by requiring that at $\bar{b} = b_{GC}(x_{max})$ the $I_{GC}(x_{max}) = I_{GC}(x = q)$. This equation can be solved analytically to give

$$q = \frac{2(1 - \bar{\Phi})^2(3\bar{\Phi} - 1)}{\bar{\Phi}(3 - 5\bar{\Phi})}, \quad \frac{1}{3} < \bar{\Phi} < \frac{1}{2}. \quad (83)$$

which is denoted as the dashed curve in Figure 7. On the right of this curve, the global minimum of the reduced action is either at $x = q$ or $x = x_{max}$. There is a critical temperature $T_0 = 1/b_0$ where the reduced action at $x = q$ and $x = x_{max}$ are equal. Below this temperature the global minimum is at $x = q$ while above it is at $x = x_{max}$. In both cases, we regard the system as unstable. On the left of the dashed curve, whether the locally stable state becomes the global minimum of the reduced

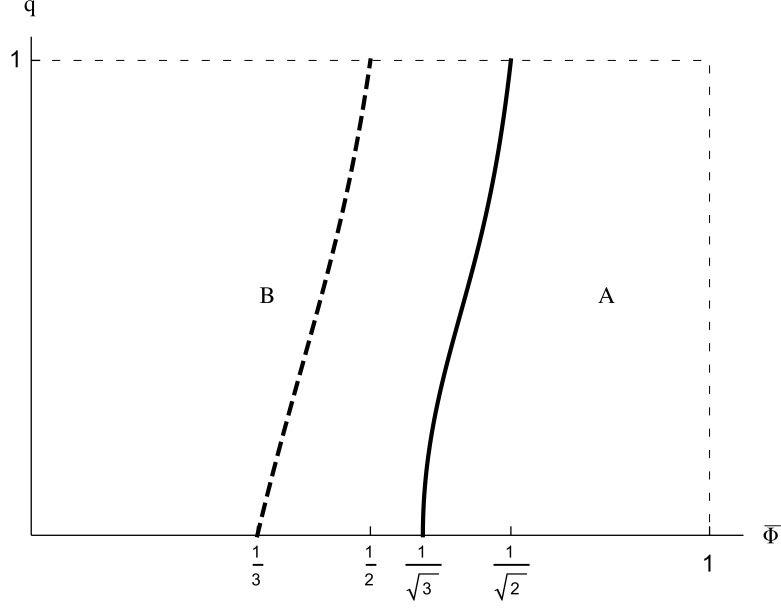


Figure 7: $q - \bar{\Phi}$ parameter plane in D2-D6 GC ensemble. Region B includes all the region on the left of the solid curve.

action depends on the temperature. There is a temperature denoted as $T_{\text{unstable}} \equiv 1/b_{\text{unstable}}$ with $b_2 < b_{\text{unstable}} < b_1$ such that the reduced action at the locally stable point equals the one at $x = q$, i.e. $I_{GC}(\bar{x}) = I_{GC}(q)$. Below this temperature, i.e. $\bar{b} > b_{\text{unstable}}$, the global minimum is still at $x = q$. Only for $b_2 < \bar{b} < b_{\text{unstable}}$, the local stability becomes a global one. For higher temperatures with $\bar{b} < b_2$, the global minimum of the reduced action is at $x = x_{max}$ and the system is unstable again.

Next for $p = 1$, at the left end $x = q$, $b_{GC}(x = q)$ has a non-vanishing finite limit which is different from GG ensemble and $p = 2$ case. Now, $g(x, q)$ can be factorized as

$$g(x, q) = (x + q)(x - q)(x - x_-)(x - x_+), \quad (84)$$

where

$$x_{\pm} = \frac{1 + 3q^2 \pm \sqrt{(1 - q^2)(1 - 9q^2)}}{4}. \quad (85)$$

One can see that for $q > 1/3$, which is region C in Figure 9, x_- and x_+ are complex conjugates and $g(x, q) > 0$, which means b_{GC} decreases monotonically for $x \in (q, x_{max})$ as shown in Figure 8(c). In this case, there is a globally stable black brane phase for $b_2 < \bar{b} < b_1$. For $q < 1/3$, it is easy to verify $x_- < q < x_+$, and therefore $g(x, q)$ is negative (b_{GC} increases) for $x \in (q, x_+)$ and is positive (b_{GC} decreases) for $x > x_+$. This indicates that if $x_+ > x_{max}$, b_{GC} is monotonically increasing (Figure 8(a)) and there is no stable black brane phase. This case is denoted as region A in Figure 9. For $x_+ < x_{max}$, the behavior of b_{GC} is shown in 8(b) and there exists a locally stable black brane phase for $b_2 < \bar{b} < b_{max}$, which is denoted as region B in Figure 9. On the boundary between A and

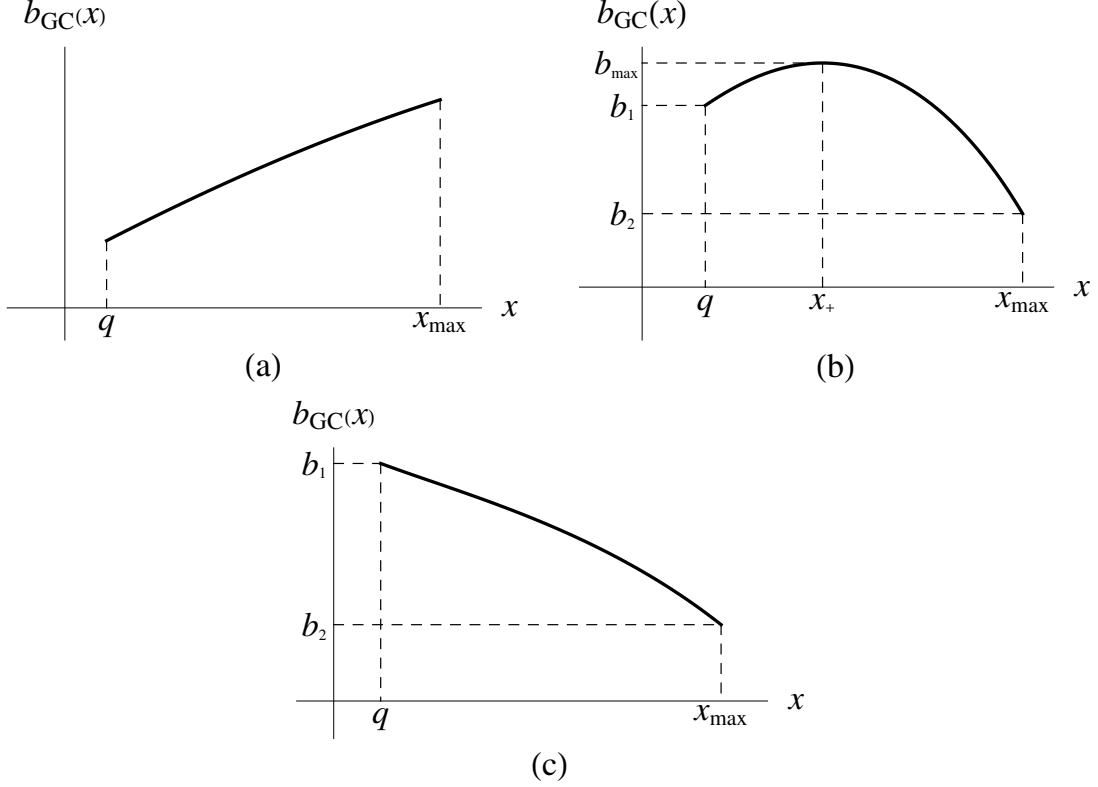


Figure 8: Typical $b_{GC}(x)$ behaviors for D1-D5 system. (a) $q < 1/3$ and $x_{max} < x_+$, corresponds to region A; (b) $q < 1/3$ and $x_{max} > x_+$, corresponds to region B; (c) $q > 1/3$, corresponds to Region C.

B, q and $\bar{\Phi}$ are related by

$$q = \frac{\sqrt{(2 - \bar{\Phi}^2)(2\bar{\Phi}^2 - 1)}}{3\bar{\Phi}}, \quad \frac{1}{\sqrt{2}} < \bar{\Phi} < 1. \quad (86)$$

In region B, like in $p = 2$ case, the locally stable black brane state may not be the global minimum and the $x = q$ point may have lower reduced action. The condition that the system is just to have only $x = q$ as the global minimum of the reduced action for all $\bar{b} > b_2$ is

$$q = \frac{1}{3}\left(5 - 2\bar{\Phi} - \frac{2}{\bar{\Phi}}\right), \quad \frac{1}{2} < \bar{\Phi} < 1, \quad (87)$$

which is also denoted as the dashed curve in Figure 9. On the right of the curve, the global minimum is either at $x = q$ for $\bar{b} > b_2$ or at $x = x_{max}$ for $\bar{b} < b_2$ and the system is regarded as unstable. On the left of the dashed curve, there is a possibility that at some temperature $T_{unstable} \equiv 1/b_{unstable}$ the reduced action at $x = q$ equals the one at the locally stable point (see Appendix E for further details on how to find this temperature). Below this temperature ($\bar{b} > b_{unstable}$), the reduced action at $x = q$ is the global minimum and the system tends to $x = q$ similar to the cases in region C and the system is also unstable. The locally stable one becomes a globally stable one only when the temperature is

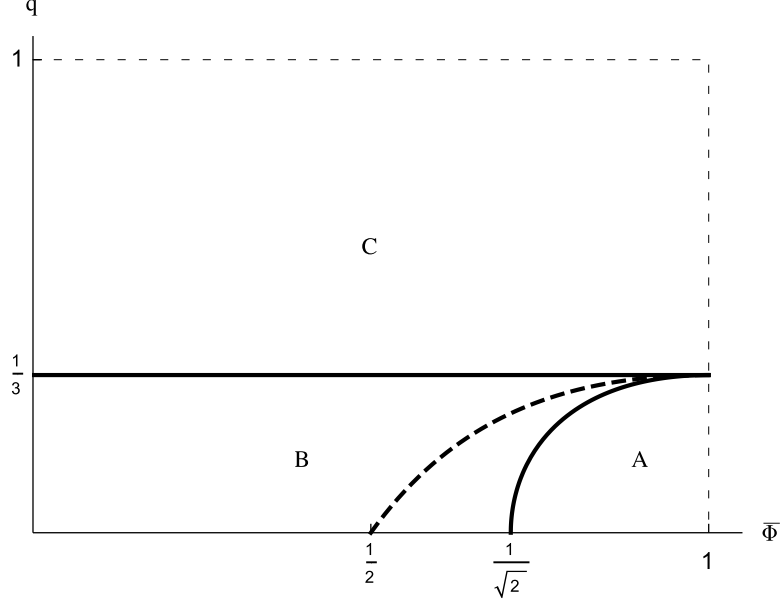


Figure 9: Parameter plane in D1-D5 GC ensemble. Region B includes all the region on the left of the solid line between A and B. The b_{GC} behaviors of A, B, C correspond to (a), (b), (c) in Figure 8.

above T_{unstable} , i.e. $b_2 < \bar{b} < b_{\text{unstable}}$. When the temperature is higher than $1/b_2$, $x = x_{\text{max}}$ becomes the global minimum of the reduced action, and so, the system becomes unstable again.

Finally, for the $p = 0$ case, there are three kinds of $b_{GC}(x)$ behaviors which are shown in Figure 3. Similar to the one-charge black $(p + 4)$ -brane case [5], there exists a critical charge q_c beyond which $b_{GC}(x)$ is a monotonically decreasing function for arbitrary $\bar{\Phi}$ as shown in Figure 3(c). When $q = q_c$ and $0 < \bar{\Phi} < \bar{\Phi}_{\text{max}}$, where $\bar{\Phi}_{\text{max}}$ is obtained in Appendix C to be $\bar{\Phi}_{\text{max}} \cong 0.871417$, b_{GC} has an inflection point at which a second order phase transition occurs. At $\bar{\Phi}_{\text{max}}$, the position of the critical point \bar{x} is equal to x_{max} . For $\bar{\Phi} > \bar{\Phi}_{\text{max}}$ at $q = q_c$, the critical point position \bar{x} is larger than x_{max} and can not be reached by the supergravity solution and hence b_{GC} is also a monotonically decreasing function. So, in $q - \bar{\Phi}$ plane, the region denoted as C in Figure 10, which contains only decreasing $b_{GC}(x)$, includes the $q > q_c$ region as well as a small region with $q < q_c$ where the solutions for $db_{GC}(x)/dx = 0$ are larger than x_{max} . In this figure, $q_c \approx 0.141626$ is the same critical value as the $\tilde{d} = 3$ case in [5] as expected. So, in region C, there is always a stable black brane phase for $\bar{b} > b_{GC}(x_{\text{max}})$. In region A and B, curves of b_{GC} have the same shape as in the other two diagrams (a) and (b) in Figure 3, respectively. On the boundary lines between A and B and between A and C, q and $\bar{\Phi}$ has following relation,

$$q = \frac{1 - \bar{\Phi}^2}{\bar{\Phi}(9 - 7\bar{\Phi}^2)} \sqrt{2(3 - \bar{\Phi}^2)(5\bar{\Phi}^2 - 3)}, \quad \sqrt{\frac{3}{5}} < \bar{\Phi} < 1. \quad (88)$$

In every region (A, B, C) there are chances for this system to have a locally stable black brane phase. In all these three cases, as $x \rightarrow q$, $db_{GC}/dx < 0$ which means that the locally stable black brane

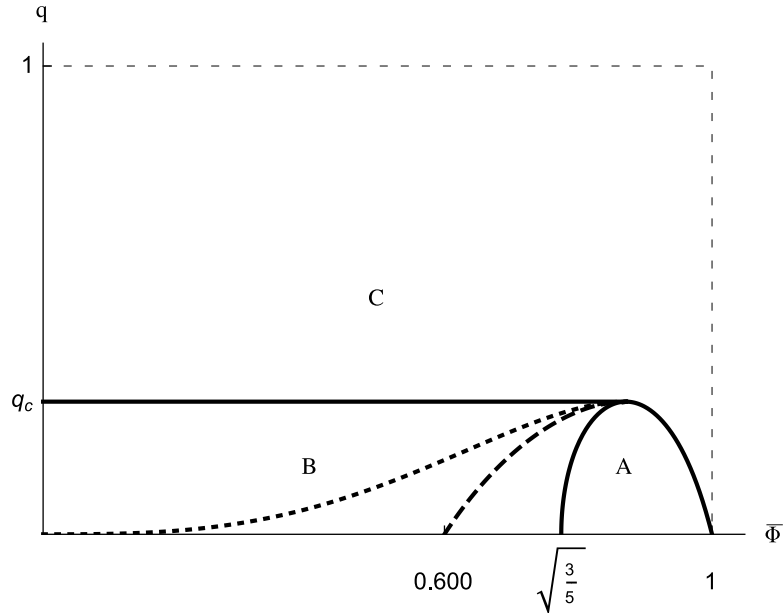


Figure 10: Parameter plane in D0-D4 GC ensemble. Region B includes all the region on the left of the solid line between A and B. The b_{GC} behaviors of A, B, C correspond to (a), (b), (c) in Figure 3.

can exist for arbitrarily small temperatures. But the minimum of b_{GC} does not tend to zero which means that at high enough temperature the locally stable black brane can not exist. In region C, at temperatures higher than $1/b_{GC}(x_{max})$, the global minimum is at x_{max} . In region A, there is a temperature $T_{unstable}$ higher than $1/b_{GC}(x_{max})$, at which the reduced action at x_{max} is equal to the one at the local minimum. When the temperature is higher than $T_{unstable}$ the global minimum is at x_{max} . Under both these two circumstances the system is unstable and we do not know what the final state is. So, in region A and region C, at temperature below $1/b_{GC}(x_{max})$ and $T_{unstable}$, respectively, the black brane is the globally stable phase. In region B which corresponds to Figure 3(b), there can also be a first order phase transition under some circumstances. As stated in section 3.1, we need to discuss two cases separately, $b_{min} > b_{GC}(x_{max})$ and $b_{min} < b_{GC}(x_{max})$ which correspond to the left and right regions of the dotted line in region B, respectively. When $b_{min} > b_{GC}(x_{max})$, the system has one locally stable black brane phase for $b_{GC}(x_{max}) < \bar{b} < b_{min}$ or $\bar{b} > b_{max}$, which is also the global minimum. For $b_{min} < \bar{b} < b_{max}$, there can be two locally stable black brane phases and the final phase should be the one with lower reduced action. There is a first-order phase transition temperature $T_t = 1/b_t$ at which the reduced actions of the two phases are equal. Above (or below) this temperature the larger (or the smaller) one is the global minimum. This is the same as the corresponding case in canonical ensemble of one-charge black brane. When $b_{min} < b_{GC}(x_{max})$, we still define a temperature $T_t \equiv 1/b_t$, at which the reduced action at the two local minima are equal even when one minimum has $\bar{x} > x_{max}$. In this case, we need to consider two subcases. The first one has $b_t > b_{GC}(x_{max})$. Then when $\bar{b} < b_{GC}(x_{max})$, i.e. the temperature higher than $1/b_{GC}(x_{max})$, the minimum of the reduced action is at $x = x_{max}$

and the system is unstable. Below this temperature, the analysis is the same as the above case and the system can have a first order transition at T_t between the two locally stable minima. The second subcase is when $b_t < b_{GC}(x_{max})$. In this subcase, at b_t the larger solution for $b_t = b_{GC}(x)$ goes beyond x_{max} and there is another temperature $T_{unstable} \equiv 1/b_{unstable} (> T_t)$ at which $I_{GC}(x_{max})$ equals the one at the local minimum with smaller \bar{x} . Then, condition for x_{max} to be the global minimum of the reduced action is $\bar{b} < b_{unstable}$. So for temperature higher than $T_{unstable}$ the system is unstable and we can not say much about the phase of the system. For $b_{GC}(x_{max}) > \bar{b} > b_{unstable}$, the smaller locally stable black brane has the lower reduced action than at $x = x_{max}$, and hence is the global minimum. So for temperature lower than $T_{unstable}$, the smaller locally stable black brane is the global minimum. The condition for $b_t = b_{GC}(x_{max})$ can only be solved numerically and is denoted as the dashed line in Figure 10. On the dashed line, $b_{unstable}$ coincides with b_t and $b_{GC}(x_{max})$. The left region of the dashed line corresponds to the $b_t > b_{GC}(x_{max})$ case which has the van der Waals-like phase structure and the right of the line in B corresponds to the $b_t < b_{GC}(x_{max})$ case.

3.4 CG ensemble

In this ensemble, we fix the Dp -brane charge Q and the potential $\bar{\varphi}$ for $D(p+4)$ at the boundary. Using the ‘‘electromagnetic’’ equilibrium equation,

$$\varphi(x, q) = \bar{\varphi}, \quad (89)$$

the reduced action of the system depends on the only variable x ,

$$\tilde{I}_{CG}(x) = \tilde{I}_{CG}(x, Q = \text{const.}, q = q_{CG}(x, \bar{\varphi})), \quad (90)$$

where q_{CG} is the solution to (89),

$$q_{CG}(x, \bar{\varphi}) = \frac{x\bar{\varphi}}{\xi^{1/2}}. \quad (91)$$

This relation also guarantees that $x > q_{CG}$ is satisfied as long as $\bar{\varphi} < 1$. At $x \rightarrow 0$, $q_{CG} \rightarrow 0$ and $\xi \rightarrow 1$. From (49), we can see that $\bar{\Delta}_- \rightarrow \bar{\Delta}_+$, which means the curvature singularity is coming closer to the horizon. Actually it can be shown that the scalar curvature blows up at the horizon $x = 0$ by explicit calculations. The quantum effect near horizon, therefore, may be large such that the semi-classical approach can not be applied. So, as in the GC ensemble, if at $x = 0$ or $x = 1$, the system has lower reduced action than the local minimum, we will consider it as unstable in the semi-classical approach.

Now we can perform the one-variable analysis by requiring

$$\frac{d\tilde{I}_{CG}(x)}{dx} = f_{CG}(x) [\bar{b} - b_{CG}(x)] = 0, \quad (92)$$

where

$$\begin{aligned} b_{CG}(x) &= b(x, Q, q_{CG}), \\ f_{CG}(x) &= \frac{\bar{\Delta}_- - \bar{\Delta}_+}{2\bar{\Delta}_+^{1/2}\bar{\Delta}_-^{1/2}(1 - \bar{\Delta}_+)} \left[5 - p + (3 - p) \frac{\bar{\Delta}_-(\bar{\Delta}_- - \bar{\Delta}_+)}{\bar{\Delta}_*\bar{\Delta}_+ + \bar{\Delta}_*\bar{\Delta}_- - 2\bar{\Delta}_+\bar{\Delta}_-} \right] > 0. \end{aligned} \quad (93)$$

Let us assume \bar{x} to be the solution of equation (92), then the minimum condition of free energy is again reduced to

$$\frac{db_{CG}(\bar{x})}{dx} < 0. \quad (94)$$

The left hand side of the above inequality is

$$\frac{db_{CG}(x)}{dx} = \frac{b_{CG}}{2(3-p)x} \left[2 - \frac{(3-p)\bar{\Delta}_-}{\bar{\Delta}_+} + \frac{(3-p)\bar{\Delta}_-(\bar{\Delta}_- - \bar{\Delta}_+)}{\bar{\Delta}_*\bar{\Delta}_+ + \bar{\Delta}_*\bar{\Delta}_- - 2\bar{\Delta}_+\bar{\Delta}_-} \right]. \quad (95)$$

One can easily check that when $Q = 0$, i.e. $\bar{\Delta}_* = \bar{\Delta}_-$, (95) automatically falls back to equation (34) in [33]. Now with (95) and the first equation in (93), we can redo all the analyses done in the two previous subsections. However, since the computations are complicated and tedious, we put the details into Appendix D for interested readers. Here we just list the final results.

For $p = 2$ case, similar to Figure 7 in GC ensemble, we have the following graph (Figure 11). In

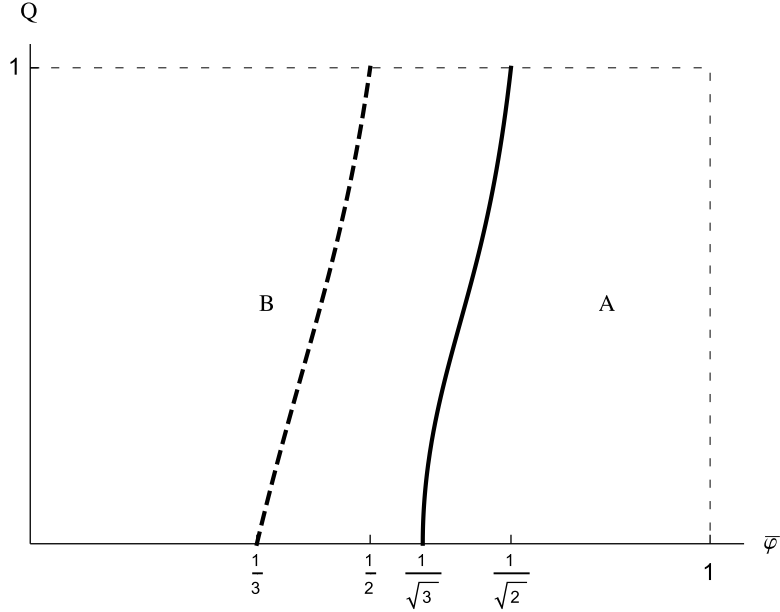


Figure 11: $Q - \bar{\varphi}$ parameter plane in D2-D6 CG ensemble

area A, since b_{CG} increases monotonically as the left graph in Figure 1, there is no stable black brane phase, while in area B, b_{CG} behaves as in Figure 4, there exists a locally stable black brane state for $b_2 < \bar{b} < b_1$. The curve separating region A and B is described by

$$Q = \frac{(-1 + \bar{\varphi}^2)\sqrt{2(1 - \bar{\varphi}^2)(3\bar{\varphi}^2 - 1)}}{\bar{\varphi}(5\bar{\varphi}^2 - 3)}, \quad \frac{1}{\sqrt{3}} < \bar{\varphi} < \frac{1}{\sqrt{2}}. \quad (96)$$

Again, the local minimum may or may not be the global minimum. It should compete with the boundary point $x = 0$ or $x = 1$. Similar to the discussion in GC ensemble, in Figure 11, on the

right of the dashed line, the local minimum can not be the global minimum of the system and on the left, it can be the global minimum for certain temperature $T \in (T_{\text{unstable}}, 1/b_2)$, where T_{unstable} is the temperature at which the reduced action at the local minimum equals the one at $x = 0$. All the discussions in the GC ensemble can be used here and we would not repeat them. The dashed line is described by

$$Q = \frac{2(1 - \bar{\varphi}^2)(3\bar{\varphi}^2 - 1)}{\bar{\varphi}(3 - 5\bar{\varphi}^2)}, \quad \frac{1}{3} < \bar{\varphi} < \frac{1}{2}. \quad (97)$$

Notice if one makes the exchanges $\bar{\Phi} \leftrightarrow \bar{\varphi}$ and $q \leftrightarrow Q$, (96) and (97) exchange with (82) and (83). So, Figure 11 is the same as Figure 7 except the labels.

For $p = 1$ case, the behaviors of $b_{CG}(x)$ are the same as the ones in GC ensemble and Figure 8 can also be used here with the only difference that the domain is now $0 < x < 1$. In the $Q - \bar{\varphi}$ plane, the three cases of (a), (b), (c) in Figure 8 correspond to region A, B, C in Figure 12. In the lower

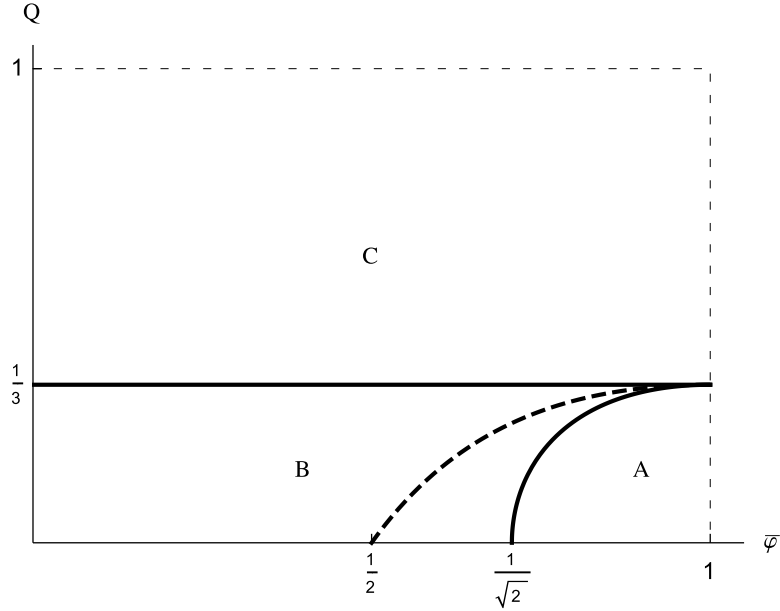


Figure 12: Parameter plane in D1-D5 CG ensemble

right region A, b_{CG} is monotonically increasing and therefore there is no stable black brane phase. In the upper half region C, since $b_{CG}(x)$ is always decreasing, there is always a locally stable black brane state for $b_{CG}(0) > \bar{b} > b_{CG}(1)$ when constant \bar{b} has an intersection point with b_{CG} curve. In the lower left region B, for $b_{CG}(1) < b < b_{max}$, where b_{max} is the maximum of b_{CG} , there will be a locally stable black brane phase since the constant \bar{b} line intersects with b_{CG} at some point where $db_{CG}/dx < 0$. The curve separating region A and region B is solved in the appendix to be

$$Q = \frac{\sqrt{(2 - \bar{\varphi}^2)(2\bar{\varphi}^2 - 1)}}{3\bar{\varphi}}, \quad \frac{1}{\sqrt{2}} < \bar{\varphi} < 1. \quad (98)$$

For the local minimum in B to be a global minimum, the system should be in the region on the left of the dashed line. On the right of the dashed line, the global minimum is either at $x = 0$ or at $x = 1$ and hence the system is unstable. On the left of the dashed line, there is a b_{unstable} between $b_{CG}(1)$ and the maximum b_{max} of b_{CG} , where the local minimum of the reduced action equals the reduced action at $x = 0$. Only for temperatures such that $b_{CG}(1) < \bar{b} < b_{\text{unstable}}$, the local minimum becomes the global minimum. The dashed line is described by

$$Q = \frac{1}{3}\left(5 - 2\bar{\varphi} - \frac{2}{\bar{\varphi}}\right), \quad \frac{1}{2} < \bar{\varphi} < 1, \quad (99)$$

One may have already found that (98) and (99) are the same as (86) and (87) except the exchanges of $q \leftrightarrow Q$ and $\bar{\Phi} \leftrightarrow \bar{\varphi}$. All the discussions of different phases are the same as the ones in GC ensemble for $p = 1$ and we will not repeat them here.

The $Q - \bar{\varphi}$ plane graph for $p = 0$ case is shown in Figure 13. In all three regions, since as $x \rightarrow 0$, b_{CG}

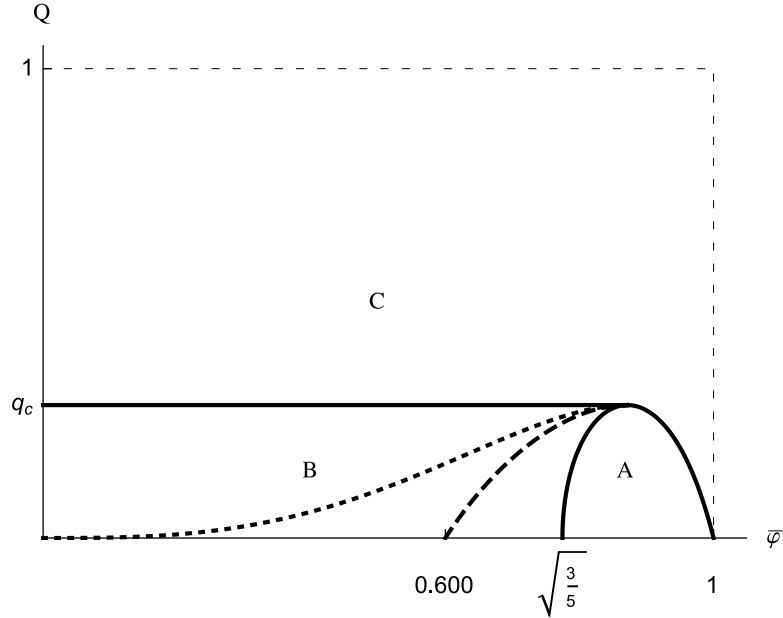


Figure 13: Parameter plane in D0-D4 CG ensemble

tends to positive infinity, there is always a stable black brane phase at arbitrarily low temperature. As long as $\bar{\varphi}$ is not zero, b_{CG} has a finite minimum, which means for high enough temperatures, the black brane can not exist. To be specific, in region C which occupies almost all valid area of the parameter plane, the behavior of b_{CG} is decreasing similar to Figure 3(c) with the domain of x replaced by $0 < x < 1$. So there is always a locally stable black brane phase for $\bar{b} > b_{CG}(1)$. In region A, which takes only a very small portion of the plane, b_{CG} behaves like Figure 3(a) which decreases first and then increases. Thus there could be a locally stable black brane phase if that solution \bar{x} is in the decreasing segment. In region B, the b_{CG} curve looks like Figure 3(b), and as discussed in the GC ensemble, there can be a van der Waals-like phase transition on the left of the dashed line in Figure 13

when the phase transition temperature $T_t = 1/b_t$ is lower than $1/b_{CG}(1)$, where b_t can be obtained by requiring the reduced actions to be equal at the two local minimum. On the right side of the dashed line, similar to what we did in the GC ensemble, we define a temperature $T_{\text{unstable}}(> T_t)$ at which the reduced action at the local minimum with smaller \bar{x} equals the one at $x = 1$. In this case, below the temperature T_{unstable} , the smaller black brane is the global minimum. For temperature higher than T_{unstable} the global minimum tends to $x = 1$ which means the instability of the system and a failure of our method. A second order phase transition can happen on the boundary line between regions B and C, when $Q = Q_c \cong 0.141626$ and $\bar{\varphi} < 0.871417$. On this line, b_{CG} has an inflection point where a second order phase transition occurs and the two phases are indistinguishable. All the detailed discussions are the same as the $p = 0$ case in GC ensemble.

As we have mentioned before, the three diagrams in this subsection are essentially the same as those in the previous subsection except that we substitute $\bar{\Phi}$ and q for $\bar{\varphi}$ and Q . Even the critical charges are precisely equal, $q_c = Q_c$. This indeed supports the statement that the Dp branes and the D(p + 4) branes are equipotent as far as only the thermodynamics is concerned, which has been pointed out in [29]. One may think of it as a symmetry,

$$\bar{\varphi} \leftrightarrow \bar{\Phi}, \quad Q \leftrightarrow q. \tag{100}$$

4 Conclusions and outlook

In this paper, we have discussed different thermodynamical ensembles of Dp-D(p + 4) system, where $p = 0, 1, 2$. The two kinds of charges can be in either canonical or grand canonical ensemble separately, so there can be CC, GG, GC, CG ensembles. CC ensemble has already been discussed in [29] and we focus on the other three ensembles in this paper. In the following we summarize the results obtained in this paper.

For GG ensemble, the potentials for Dp and D(p + 4) are fixed. At very low temperature, the hot flat space is the stable phase. Depending on the values of $\bar{\Phi}$ and $\bar{\varphi}$, at higher temperatures black brane phase may or may not be a globally stable phase. For larger $\bar{\Phi}$ or $\bar{\varphi}$ which satisfies (68), black brane can not be a globally stable phase. In this case, below T_{unstable} the globally stable phase is the hot flat space and above it the horizon of the system approaches the boundary and the quantum effect will be important, therefore we do not know what happens in this system under these circumstances. In this case, the system is regarded as unstable in our semi-classical approach. Only for small $\bar{\Phi}$ and $\bar{\varphi}$ satisfying (69), the black brane can be a globally stable phase at temperature $T \in (T_0, 1/b(x_{max}))$. At much higher temperatures, like in case A, the horizon of the system also tends to the boundary and the black brane is unstable. As in most grand canonical systems, there is no van der Waals-like phase transition.

For GC ensemble, in which the D(p + 4) charge q and Dp potential $\bar{\Phi}$ are fixed, the D2-D6, D1-D5 and D0-D4 behave differently. In D2-D6 system, on the right side of the dashed line in Figure 7, the global minimum of the reduced action is either at $x = q$ or at $x = x_{max}$, and the black brane can not

be a stable phase. On the left of the dashed line, in a comparably small region of $\bar{\Phi}$, the black brane phase can be the final stable phase only when the temperature is in range $(T_{\text{unstable}}, 1/b_{GC}(x_{\text{max}}))$. Below or above this range, the global minimum is at $x = q$ or $x = x_{\text{max}}$, respectively, and the system is thus unstable. For D1-D5 system, in the region below $q_c = 1/3$ in Figure 7, the discussion is similar to the D2-D6 system. For the region above q_c , the black brane is always the final stable phase for temperature lower than $1/b_{GC}(x_{\text{max}})$ and higher than $1/b_{GC}(q)$. For higher or lower temperatures, the global minimum for the reduced action is at $x = x_{\text{max}}$ or $x = q$ which means the instability of the system. For D0-D4 system, there can be a van der Waals-like first order phase transition between a small black brane and a larger one in the region on the left of the dashed line in region B in Figure 10, which is below the critical charge q_c at which a second order phase transition happens. The critical charge is independent of $\bar{\Phi}$ and is the same as the one for the black D4-brane in the canonical ensemble. Below the first order phase transition temperature T_t (or above T_t and below $1/b(x_{\text{max}})$), the final system is in a small black brane phase (or a large one). For higher temperatures, the global minimum is at $x = x_{\text{max}}$ again, which means that the system is unstable and is beyond our approach to handle. In the region on the right of the dashed line in B, or in region A, for temperatures below T_{unstable} or $1/b(x_{\text{max}})$, respectively, the black brane is always the final stable phase, though there may be a larger metastable one in the corresponding part in region B for some temperature $T \in (1/b_{\text{max}}, 1/b(x_{\text{max}}))$. In region C, for temperatures lower than $1/b(x_{\text{max}})$, the final stable phase is always the black brane.

The fact that the critical charge q_c in D0-D4 GC ensemble is independent of $\bar{\Phi}$ is an unexpected result. Notice that according to (72), Q_{GC} still depends on $\bar{\Phi}$ non-trivially. Recall that for extremal Dp - $D(p+4)$ branes satisfying the Harmonic function rules and preserving 1/4 supersymmetries, there is no binding energy[34], which means that the two kinds of charges do not affect each other. However, we are considering non-extremal cases here, and the two kinds of charges must be correlated, which is already demonstrated in the CC ensemble where the critical line correlates both charges as in Figure 14. Whether this independence of $\bar{\Phi}$ of the critical charge in GC ensemble means that something special happens in such a critical condition is an interesting problem for future work.

From above discussion, we can see that D2-D6 GC ensemble behaves more like GG ensemble. The b_{GC} and b_{GG} have the same behavior as described by Figure 1 and changes similarly as we tune the $\bar{\Phi}$ in both GC ensemble and GG ensemble at small $\bar{\varphi}$. The difference is that at $x = 0$ in grand canonical ensemble there is the hot flat space but at $x = q$ in GC ensemble the extremal black brane has naked singularity and our method fails. There could be new phases emerging around $x = q$ in GC ensemble like hot flat space in GG ensemble due to quantum effects. D0-D4 GC ensemble is more like the canonical ensemble. There can be a van der Waals-like phase transition and there is a critical charge. Tuning q is similar to that in the one-charge black brane canonical ensemble for small $\bar{\Phi}$. But for large $\bar{\Phi}$ the van der Waals-like phase transition may disappear.

The CG case is almost the same as GC case except for the exchanges in $q \leftrightarrow Q$ and $\bar{\Phi} \leftrightarrow \bar{\varphi}$. As in the CC ensemble [29], the phase structure of the GG ensemble is already symmetric by itself under this transformation. So the smeared Dp charges and the $D(p+4)$ charges in the Dp - $D(p+4)$ system

are equipotent as long as only the thermodynamic properties are considered, which may be a hint for some underlying symmetry.

Appendices

A Phase structures in CC ensemble

Compared with the other ensembles, the analysis in CC ensemble is much simpler due to the fact that both charges Q and q are fixed, which leads to the consequence that

$$b_{CC}(1) = 0. \tag{101}$$

Hence the shape of Figure 3 (a) would never occur, i.e., systems that have van der Waals-like structures can only have $b_{CC}(x)$ with shapes shown in Figure 3 (b) and (c). Therefore, there is only one transition line in the $Q - q$ plane which is also the critical line on which a second order phase transition occurs. However, unlike in GC or CG ensemble where only D0-D4 can have van der Waals-like phase transitions, in CC ensemble, both D0-D4 and D1-D5 can have this behavior. In Figure 14 we show the critical lines in $Q - q$ parameter plane. In both diagrams, B corresponds to the region where $b_{CC}(x)$ is a monotonically decreasing function and A corresponds to the region where van der Waals-like phase transition can happen. In D0-D4 case, the critical line intersects with the coordinate axes at $Q_c = q_c = 0.141626$, which exactly matches the result in the presence of only Dp or $D(p + 4)$ charges [5].

For D2-D6 system, there are no critical behaviors. However, depending on where (Q, q) pair lies in the $Q - q$ plane there still can be two possible shapes of $b_{CC}(x)$, as shown in Figure 15. The diagram for $Q - q$ plane is shown in Figure 16, in which region A corresponds to the left diagram in Figure 15 and region B corresponds to the right one. The boundary line between these two regions can be obtained analytically to be

$$q = \frac{Q}{4Q - 1} \quad \text{or} \quad Q = \frac{q}{4q - 1}, \tag{102}$$

where $\frac{1}{3} < Q, q < 1$, which shows the symmetry between charge Q and q .

B The condition for globally stable black brane phases in the GG ensemble

When $x = \bar{x}$ we have

$$\tilde{I}_{GG} = \frac{5-p}{3-p} \left(\frac{\bar{x}}{1-\bar{\Phi}^2} \right)^{1/2} \frac{(1-\bar{\xi})^{\frac{1}{2} + \frac{1}{3-p}}}{1+\bar{\xi}^{1/2}} \left(\bar{\xi}^{1/2} - \frac{3-p}{5-p} \right), \tag{103}$$

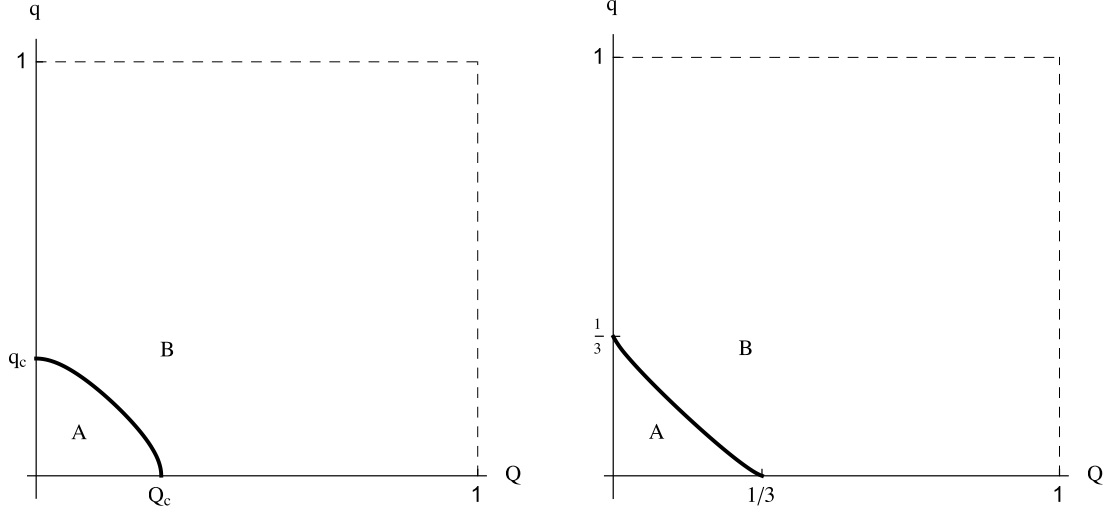


Figure 14: Critical lines in CC ensemble. The left diagram corresponds to D0-D4 case and the right one corresponds to D1-D5 case. The right diagram has already been shown in [29]. Both critical lines are computed numerically.

where $\bar{\xi} = 1 - \bar{x}(1 - \bar{\varphi}^2)$. Now we need to find out when $\tilde{I}_{GG} < 0$, or when

$$\bar{\xi} < \left(\frac{3-p}{5-p} \right)^2. \quad (104)$$

This leads to the condition that

$$\bar{x} > \bar{x}_0(\bar{\varphi}) = \frac{4(4-p)}{(5-p)^2} \frac{1}{1-\bar{\varphi}^2} \quad \text{or} \quad \bar{b} < b_{GG}(\bar{x}_0(\bar{\varphi})). \quad (105)$$

However, we have a restriction for \bar{x} which is $x_0 < \bar{x} < x_{max}$. That means only if $\bar{x}_0(\bar{\varphi}) < x_{max}$ we can have $\bar{x} > \bar{x}_0(\bar{\varphi})$. It is easy to check that $\bar{x}_0(\bar{\varphi}) > x_0$ is automatically satisfied, whereas for $\bar{x}_0(\bar{\varphi}) < x_{max}$ to hold we need

$$\max\{\bar{\Phi}, \bar{\varphi}\} < \frac{3-p}{5-p}. \quad (106)$$

Thus we find the condition for the black brane phase to be globally stable,

$$\max\{\bar{\Phi}, \bar{\varphi}\} < \frac{3-p}{5-p} \quad \text{and} \quad \bar{b} < b_{GG}(\bar{x}_0(\bar{\varphi})). \quad (107)$$

C Parameter planes in GC ensemble

We have argued in section 3.3 that we can find the transition lines between region A and region B in Figure 7 for $p = 2$ by setting the b_{GC} curve at the right end point to be flat. This can also be used in arbitrary p . That is,

$$g(x_{max}, q) = 0, \quad (108)$$

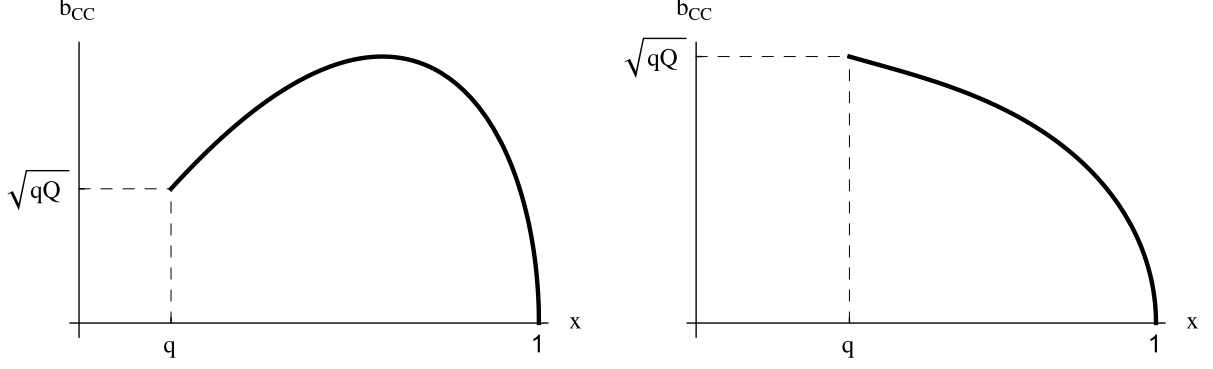


Figure 15: Possible shapes of $b_{CC}(x)$ for D2-D6-brane in CC ensemble.

where x_{max} satisfies following equation (see (74)),

$$x_{max}^2 - (1 - \bar{\Phi}^2)x_{max} - q^2\bar{\Phi}^2 = 0. \quad (109)$$

The above quadratic equation has two solutions and x_{max} is the larger one. Therefore, there is another restriction on x_{max} ,

$$x_{max} > \frac{1 - \bar{\Phi}^2}{2} \quad (110)$$

From (109), we can express q through x_{max} ,

$$q^2 = \frac{x_{max}^2 - (1 - \bar{\Phi}^2)x_{max}}{\bar{\Phi}^2}. \quad (111)$$

Putting this relation into (108), we can factorize $g(x_{max}, q)$ as follows,

$$g(x_{max}, q) = \frac{x_{max}^2(1 - x_{max})^2}{2\bar{\Phi}^4} \left\{ [3(3 - p) - (7 - p)\bar{\Phi}^2] x_{max} - 2(3 - p - \bar{\Phi}^2)(1 - \bar{\Phi}^2) \right\}. \quad (112)$$

Thus we find the relation between x_{max} and $\bar{\Phi}$ when (108) is satisfied,

$$x_{max} = \frac{2(3 - p - \bar{\Phi}^2)(1 - \bar{\Phi}^2)}{3(3 - p) - (7 - p)\bar{\Phi}^2}. \quad (113)$$

Combining (111) and (113), we finally reaches the relation between q and $\bar{\Phi}$,

$$q = \frac{1 - \bar{\Phi}^2}{\bar{\Phi} |3(3 - p) - (7 - p)\bar{\Phi}^2|} \sqrt{2(3 - p - \bar{\Phi}^2)[(5 - p)\bar{\Phi}^2 - (3 - p)]}. \quad (114)$$

From (113) and (110), the restriction on x_{max} becomes a restriction on $\bar{\Phi}$,

$$\bar{\Phi} < \sqrt{\frac{3(3 - p)}{7 - p}}. \quad (115)$$

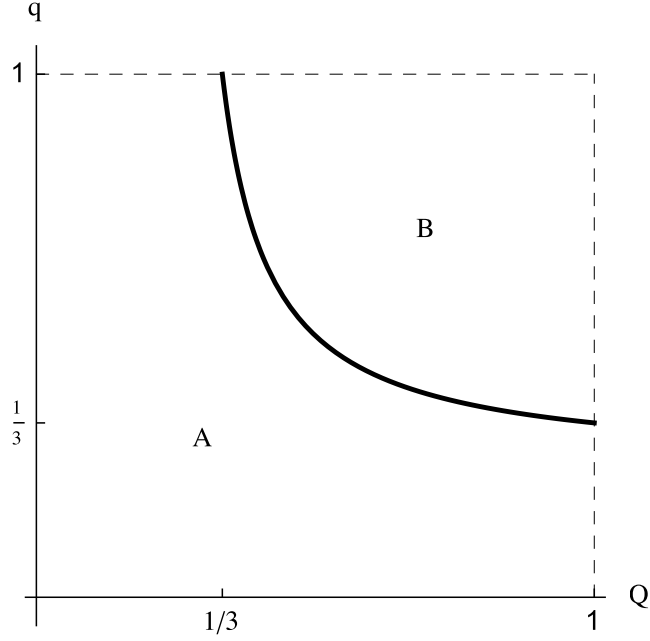


Figure 16: $Q - q$ plane for D2-D6-brane in CC ensemble.

For $p = 0$ or 1 , this restriction is satisfied automatically since $\bar{\Phi} < 1$ while for $p = 2$, this inequality reduces to $\bar{\Phi} < \sqrt{3/5}$. Now it is easy to see that, for $p = 0$ or 1 , (114) reduces to (88) or (86) and for $p = 2$ together with (115) this recovers (82).

For $p = 1$, there is another transition line between region B and region C in Figure 9 which appears when the b_{GC} curve becomes flat at the left end point. That is equivalent to setting

$$\frac{db_{GC}(q)}{dx} = -\frac{(q - 1/3)^2}{q^2(1 - q)^2} b_{GC}(q) = 0. \quad (116)$$

This gives a condition which is independent of $\bar{\Phi}$,

$$q = 1/3. \quad (117)$$

So the transition line is the horizontal line shown in Figure 9.

For $p = 0$, there is a critical line between region A and C on which the b_{GC} has a inflection point and the first and second order derivatives of b_{GC} vanishes at the same point \bar{x} . That means, we only need to combine two equations,

$$\begin{aligned} g(\bar{x}, q) &= 0, \\ \frac{\partial g(\bar{x}, q)}{\partial x} &= 0. \end{aligned} \quad (118)$$

This set of equations are solved by

$$\bar{x} \cong 0.292675, \quad q_c \cong 0.141626. \quad (119)$$

Since $x < x_{max}$, this critical point exists only when $x_{max} > \bar{x}$, which means there is an upper bound for $\bar{\Phi}$,

$$\bar{\Phi}_{max} \cong 0.871417. \quad (120)$$

D Parameter planes in CG ensemble

We have argued that the behavior of $b_{CG}(x)$ depends on the signature of $b'_{CG}(x)$. Hence we need to find the zero points of $b'_{CG}(x)$. With (91), one can easily find following relations,

$$\begin{aligned} \bar{\Delta}_- &= \frac{\bar{\Delta}_+}{\xi}, \\ \bar{\Delta}_* &= \frac{\lambda}{\xi} \bar{\Delta}_+, \end{aligned} \quad (121)$$

where

$$\begin{aligned} \xi &= 1 - (1 - \bar{\varphi}^2)x, \\ \lambda &= \frac{1 + \xi + \sqrt{(1 - \xi)^2 + 4Q^2\xi}}{2(1 - Q^2)}. \end{aligned} \quad (122)$$

With this relation one can evaluate $b'_{CG}(x)$ and set it to zero,

$$b'_{CG}(x) = \frac{b_{CG}}{2(3-p)x} \frac{\xi[3(3-p) - (7-p)\xi] - \lambda(\xi+1)(3-p-2\xi)}{\xi(\xi\lambda + \lambda - 2\xi)} = 0, \quad (123)$$

which results in,

$$\lambda = \frac{\xi[3(3-p) - (7-p)\xi]}{(\xi+1)(3-p-2\xi)}. \quad (124)$$

The second definition in (122) is equivalent to requiring

$$0 = (1 - Q^2)\lambda^2 - (1 + \xi)\lambda + \xi, \quad \text{and} \quad \lambda > \frac{1 + \xi}{2(1 - Q^2)}, \quad (125)$$

by the same token of (109) and (110). Combining (124) and (125), one gets

$$\begin{aligned} Q &= \frac{1 - \xi}{3(3-p) - (7-p)\xi} \sqrt{\frac{2(3-p-\xi)[(5-p)\xi - (3-p)]}{\xi}}, \\ \xi &< \begin{cases} 1, & \text{for } p = 0, 1 \\ \frac{3}{5}, & \text{for } p = 2 \end{cases}. \end{aligned} \quad (126)$$

By the same spirit of the previous appendix section, we examine when the slope at each end point of b_{CG} curve changes its signature. That is to set $x = 0$ and $x = 1$ for left and right end points respectively. For $x = 0$ to be the stationary point, or equivalently at $\xi = 1$, which only makes sense

when $p = 1$ (because only this case we have finite limit of b_{CG}), we have $Q = 1/3$. This corresponds to the horizontal line in Figure 12. For $x = 1$, or equivalently $\xi = \bar{\varphi}^2$, we get

$$Q = \frac{1 - \bar{\varphi}^2}{3(3 - p) - (7 - p)\bar{\varphi}^2} \sqrt{\frac{2(3 - p - \bar{\varphi}^2)[(5 - p)\bar{\varphi}^2 - (3 - p)]}{\bar{\varphi}^2}} \quad (127)$$

and $\bar{\varphi} < \sqrt{\frac{3}{5}}$ for $p = 2$. This relation represents all curves in Figure 11, 12 and 13.

Finally, we calculate the critical charge Q_c for the $p = 0$ case. From (126) we know that

$$Q_c = \frac{1 - \xi}{9 - 7\xi} \sqrt{\frac{2(3 - \xi)(5\xi - 3)}{\xi}}. \quad (128)$$

Another critical condition is that $b''_{CG}(x) = 0$. Since

$$b''_{CG}(x) \Big|_{b'_{CG}(x)=0} \sim (4\xi - 1)\lambda - (14\xi - 9) + \frac{(\xi + 1)(2\xi - 3)(\lambda - 1)}{2(1 - Q_c^2)\lambda - 1 - \xi}, \quad (129)$$

we find another equation for Q_c ,

$$2(1 - Q_c^2) = \frac{(\xi + 1)^2(2\xi - 3)}{\xi(7\xi - 9)} \left[1 + \frac{(\xi - 1)(2\xi - 3)(5\xi - 3)}{(\xi - 3)(11\xi - 9)} \right]. \quad (130)$$

Combining (128) and (130), we get only one sensible solution

$$\xi_c \cong 0.759367, \quad Q_c \cong 0.141626. \quad (131)$$

This also says that, on the critical line, x and $\bar{\varphi}$ are related through a simple formula,

$$x = \frac{1 - \xi_c}{1 - \bar{\varphi}^2} \cong \frac{0.240633}{1 - \bar{\varphi}^2}. \quad (132)$$

Since $x < 1$, this formula also indicates that $\bar{\varphi}$ has a maximal value beyond which Q_c does not exist, i.e., $\bar{\varphi}_{max} = \sqrt{\xi_c} \cong 0.871417$.

E $b_{unstable}$ in GC ensemble and the dashed lines in Figure 7 and 9

Our starting point is to find the critical $\bar{b} = b_{unstable}$ above which we have $I_{GC}(q) < I_{GC}(\bar{x})$ and the system at $x = \bar{x}$ is not globally stable. As a bonus of this process we will find the dashed lines in Figure 7 and 9. When $\bar{b} = b_{unstable}$ we have

$$\tilde{I}_{GC}(q) = \tilde{I}_{GC}(\bar{x}) \quad (133)$$

where \bar{x} takes the value such that

$$\bar{b} = b(\bar{x}). \quad (134)$$

In (133) the left and right hand side can be evaluated,

$$\begin{aligned}
\tilde{I}_{GC}(q) &= (3-p)\bar{b}q, \\
\tilde{I}_{GC}(\bar{x}) &= \bar{b} \left[8 - 2p - (5-p) \left(\frac{\bar{\Delta}_+(\bar{x})}{\bar{\Delta}_-(\bar{x})} \right)^{1/2} - (3-p) (\bar{\Delta}_+(\bar{x})\bar{\Delta}_-(\bar{x}))^{1/2} \right] \\
&\quad - \left(\frac{\bar{x}}{1-\bar{\Phi}^2} \right)^{1/2} \left(1 - \frac{\bar{\Delta}_+(\bar{x})}{\bar{\Delta}_-(\bar{x})} \right)^{3/2} \\
&= \bar{b} \left[8 - 2p - 2 \left[\frac{\bar{\Delta}_+(\bar{x})}{\bar{\Delta}_-(\bar{x})} \right]^{\frac{1}{2}} - (3-p) [\bar{\Delta}_+(\bar{x})\bar{\Delta}_-(\bar{x})]^{\frac{1}{2}} - (3-p) \left[\frac{\bar{\Delta}_-(\bar{x})}{\bar{\Delta}_+(\bar{x})} \right]^{\frac{1}{2}} \right] \quad (135)
\end{aligned}$$

where we have used (43) (71) (72) and (134) to obtain the final expressions. Combining (133) and (135) we get an equation of \bar{x} ,

$$8 - 2p - 2 \left[\frac{\bar{\Delta}_+(\bar{x})}{\bar{\Delta}_-(\bar{x})} \right]^{\frac{1}{2}} - (3-p) [\bar{\Delta}_+(\bar{x})\bar{\Delta}_-(\bar{x})]^{\frac{1}{2}} - (3-p) \left[\frac{\bar{\Delta}_-(\bar{x})}{\bar{\Delta}_+(\bar{x})} \right]^{\frac{1}{2}} = (3-p)q \quad (136)$$

That is, given any pair of $(\bar{\Phi}, q)$ we can solve (at least numerically) the above equation to find the \bar{x} that makes $\tilde{I}_{GC}(q)$ and $\tilde{I}_{GC}(\bar{x})$ equal. One can easily see that $\bar{x} = q$ is always a solution to this equation which is not the solution we want. However, it can be shown that if there exists a solution other than q , this solution is unique and therefore there exists a unique $b_{\text{unstable}} = b(\bar{x})$. Consequently, there may be regions and boundaries thereof in the q - $\bar{\Phi}$ plane within which this solution always exists. These regions should lie in region B of Figure 7 and 9 and the boundaries are exactly the dashed lines in these figures. We have argued that there is an upper limit for x which is x_{max} defined in (74), therefore on the boundary we have $\bar{x} = x_{\text{max}}$. Bringing this specific value of \bar{x} in (136), we find

$$q = \frac{2}{3-p} \frac{(1-\bar{\Phi})(3-p-\bar{\Phi})[(5-p)\bar{\Phi} - (3-p)]}{\bar{\Phi}[3(3-p) - (7-p)\bar{\Phi}]}. \quad (137)$$

Setting $p = 2$ and $p = 1$ respectively we would recover the expected functions in (83) and (87).

F Acknowledgments

This work is supported by the National Natural Science Foundation of China under grant No. 11105138, and 11235010. Z.X is also partly supported by the Fundamental Research Funds for the Central Universities under grant No. WK2030040020. D.Z is partly supported by the Chinese Scholarship Council. He would also like to thank Chao Wu, Wei Gu and Jianfei Xu for their helpful discussions as well as Prof. Yang-Hui He and City University London for providing him with a one-year visiting studentship.

References

- [1] E. Witten, *Anti-de Sitter space, thermal phase transition, and confinement in gauge theories*, *Adv. Theor. Math. Phys.* **2** (1998) 505 [hep-th/9803131].

- [2] J. W. York, *Black hole thermodynamics and the Euclidean Einstein action*, *Phys. Rev. D* **33**, 2092 (1986).
- [3] B. F. Whiting and J. W. York, Jr., *Action Principle and Partition Function for the Gravitational Field in Black Hole Topologies*, *Phys. Rev. Lett.* **61** (1988) 1336.
- [4] H. W. Braden, J. D. Brown, B. F. Whiting and J. W. York, *Charged black hole in a grand canonical ensemble*, *Phys. Rev. D* **42**, 3376 (1990).
- [5] J. X. Lu, Shibaji Roy and Zhiguang Xiao, *Phase transitions and critical behavior of black branes in canonical ensemble*, *JHEP* **01** (2011) 133, [arXiv:1010.2068v1[hep-th]].
- [6] A. Chamblin, R. Emparan, C. V. Johnson and R. C. Myers, *Charged AdS black holes and catastrophic holography*, *Phys. Rev. D* **60**, 064018 (1999) [arXiv:hep-th/9902170].
- [7] A. Chamblin, R. Emparan, C. V. Johnson and R. C. Myers, *Holography, thermodynamics and fluctuations of charged AdS black holes*, *Phys. Rev. D* **60**, 104026 (1999) [arXiv:hep-th/9904197].
- [8] S. Carlip and S. Vaidya, *Phase transitions and critical behavior for charged black holes*, *Class. Quant. Grav.* **20** (2003) 3827 [arXiv:gr-qc/0306054].
- [9] A. P. Lundgren, *Charged black hole in a canonical ensemble*, *Phys. Rev. D* **77**, 044014 (2008) [arXiv:gr-qc/0612119].
- [10] E. Witten, *Instability of the Kaluza-Klein Vacuum*, *Nucl. Phys. B* **195** (1982) 481.
- [11] G. T. Horowitz, *Tachyon condensation and black strings*, *JHEP* **08** (2005) 091 [arXiv:hep-th/0506166].
- [12] J. X. Lu, S. Roy, Z. Xiao, *The enriched phase structure of black branes in canonical ensemble*, *Nucl. Phys. B* **854** (2012) 913-925. [arXiv:1105.6323 [hep-th]].
- [13] C. Wu, Z. Xiao and J. Xu, *Bubbles and Black Branes in Grand Canonical Ensemble*, *Phys. Rev. D* **85** (2012) 044009 [arXiv:1108.1347 [hep-th]].
- [14] T. K. Dey, S. Mukherji, S. Mukhopadhyay and S. Sarkar, *Phase transitions in higher derivative gravity and gauge theory: R-charged black holes*, *JHEP* **09** (2007) 026 [arXiv:0706.3996 [hep-th]].
- [15] D. Anninos and G. Pastras, *Thermodynamics of the Maxwell-Gauss-Bonnet anti-de Sitter Black Hole with Higher Derivative Gauge Corrections*, *JHEP* **07** (2009) 030 [arXiv:0807.3478 [hep-th]].
- [16] D. C. Zou, Y. Liu and B. Wang, *Critical behavior of charged Gauss-Bonnet AdS black holes in the grand canonical ensemble*, *Phys. Rev. D* **90** (2014) 044063 [arXiv:1404.5194 [hep-th]].
- [17] C. G. Callan and J. M. Maldacena, *D-brane approach to black hole quantum mechanics*, *Nucl. Phys. B* **472** (1996) 591 [hep-th/9602043].

- [18] K. Behrndt, E. Bergshoeff and B. Janssen, *Intersecting d-branes in ten-dimensions and six-dimensions*, *Phys. Rev. D* **55** (1997) 3785 [hep-th/9604168].
- [19] G. Papadopoulos and P. K. Townsend, *Kaluza-Klein on the brane*, *Phys. Lett. B* **393** (1997) 59 [hep-th/9609095].
- [20] A. W. Peet, *TASI lectures on black holes in string theory*, [hep-th/0008241].
- [21] Y. G. Miao and N. Ohta, *Complete intersecting nonextreme p-branes*, *Phys. Lett. B* **594** (2004) 218 [hep-th/0404082].
- [22] H. Liu and A. A. Tseytlin, *D3-brane D instanton configuration and N=4 superYM theory in constant selfdual background*, *Nucl. Phys. B* **553** (1999) 231 [hep-th/9903091].
- [23] J. L. F. Barbon and A. Pasquinucci, *Aspects of instanton dynamics in AdS / CFT duality*, *Phys. Lett. B* **458** (1999) 288 [hep-th/9904190].
- [24] K. Suzuki, *D0 - D4 system and QCD(3+1)*, *Phys. Rev. D* **63** (2001) 084011 [hep-th/0001057].
- [25] C. Wu, Z. Xiao and D. Zhou, *Sakai-Sugimoto model in D0-D4 background*, *Phys. Rev. D* **88** (2013) 2, 026016 [arXiv:1304.2111 [hep-th]].
- [26] W. Cai, C. Wu and Z. Xiao, *Baryons in the Sakai-Sugimoto model in the D0-D4 background*, *Phys. Rev. D* **90** (2014) 10, 106001 [arXiv:1410.5549 [hep-th]].
- [27] S. Seki and S. J. Sin, *A New Model of Holographic QCD and Chiral Condensate in Dense Matter*, *JHEP* **1310** (2013) 223 [arXiv:1304.7097 [hep-th]].
- [28] J. J. Friess and S. S. Gubser, *Instabilities of D-brane bound states and their related theories*, *JHEP* **11** (2005) 040 [hep-th/0503193].
- [29] J. X. Lu, Ran Wei, Jianfei Xu *The phase structure of black D1/D5 (F/NS5) system in canonical ensemble*, *JHEP* **12** (2012) 012, [arXiv:1210.0708[hep-th]].
- [30] G. W. Gibbons and S. W. Hawking, *Action integrals and partition functions in quantum gravity*, *Phys. Rev. D* **15**, 2752 (1977).
- [31] S. W. Hawking, *Particle Creation by Black Holes*, *Commun. Math. Phys.* **43** (1975) 199-220.
- [32] J. M. Bardeen, B. Carter, S. W. Hawking, *The four laws of black hole mechanics*, *Commun. Math. Phys.* **31** (1973) 161-170.
- [33] J. X. Lu, Shibaji Roy and Zhiguang Xiao, *Phase structure of black branes in grand canonical ensemble* *JHEP* **05** (2011) 091, [arXiv:1011.5198[hep-th]].
- [34] A. A. Tseytlin, *'No force' condition and BPS combinations of p-branes in eleven-dimensions and ten-dimensions*, *Nucl. Phys. B* **487** (1997) 141 [hep-th/9609212].